

**Structure-Based Function Prediction of
Functionally Unannotated Structures in the PDB**
*Prediction of ATP, GTP, Sialic Acid, Retinoic Acid and
Heme-bound and -Unbound (Free) Nitric Oxide Protein Binding Sites*

Vicente M. Reyes, Ph.D.*

E-mail: vmrsbi.RIT.biology@gmail.com

*work done at:

Dept. of Pharmacology, School of Medicine,
University of California, San Diego
9500 Gilman Drive, La Jolla, CA 92093-0636
&

Dept. of Biological Sciences, School of Life Sciences
Rochester Institute of Technology
One Lomb Memorial Drive, Rochester, NY 14623

Abstract: Due to increased activity in high-throughput structural genomics efforts around the globe, there has been a steady accumulation of experimentally solved protein 3D structures lacking functional annotation, thus creating a need for structure-based protein function assignment methods. Computational prediction of ligand binding sites (LBS) is a well-established protein function assignment method. Here we apply the specific ligand binding site detection algorithm we recently described (Reyes, V.M. & Sheth, V.N., 2011; Reyes, V.M., 2015a) to some 801 functionally unannotated experimental structures in the Protein Data Bank by screening for the binding sites of six biologically important ligands, namely: GTP in small Ras-type G-proteins, ATP in ser/thr protein kinases, sialic acid, retinoic acid, and heme-bound and unbound (free) nitric oxide. Validation of the algorithm for the GTP- and ATP-binding sites has been previously described in detail (ibid.); here, validation for the binding sites of the four other ligands shows both good specificity and sensitivity. Of the 801 structures screened, eight tested positive for GTP binding, 61 for ATP binding, 35 for sialic acid binding, 132 for retinoic acid binding, 33 for heme-bound nitric oxide binding, and 10 for free nitric oxide binding. Using the ‘cutting plane’ and ‘tangent sphere’ methods we described previously, (Reyes, V.M., 2015b), we also determined the depth of burial of the ligand binding sites detected above and compared the values with those from the respective training structures, and the degree of similarity between the two values taken as a further validation of the predicted LBSs. Applying this criterion, we were able to narrow down the predicted GTP-binding proteins to two, the ATP-binding proteins to 13, the sialic acid-binding proteins to two, the retinoic acid-binding proteins to 14, the heme-bound NO-binding proteins to four, and the unbound NO-binding proteins to one. We believe this further criterion increases the confidence level of our LBS predictions. The next logical step would be the experimental determination of the actual binding of these putative proteins to their respective ligands.

Keywords: GTP binding site/proteins, ATP binding site/proteins, sialic acid binding site/proteins, retinoic acid binding site/proteins, heme-NO binding site/proteins, unbound NO binding site/proteins, protein function prediction, protein function annotation, protein-ligand interaction(s)

Abbreviations: BS, binding site; LBS, ligand binding site; PDB, Protein Data Bank; GTP, guanosine triphosphate; ATP, adenosine triphosphate; SRGP, small Ras-type G-proteins; STPK, ser/thr protein kinase; SIA, sialic acid; REA, retinoic acid; NO, nitric oxide; hNO, heme-bound NO; fNO, free or unbound NO; PLI, protein ligand interaction(s); 3D SM, 3-dimensional search motif; CP, cutting plane; CPM, CP method; TS, tangent sphere; TSM, TS method; CPi, cutting plane index; TSi, tangent sphere index; H-bond, hydrogen bond; VDW, van der Waals; AAR, all-atom representation; DCRR, double-centroid reduced representation; Z(s), the side-chain centroid of amino acid Z; X(b), the backbone centroid of amino acid X; DCRR, double-centroid reduced representation

1 Introduction.

Progress in both the genomic sequencing efforts around the globe (Burley, S.K. 2000; Heinemann, U. 2000; Terwilliger, T.C., 2000; Norrvell, J.C., & Machalek, A.Z., 2000) as well as that of the various high-throughput 3D structure-determination methods (experimental or predicted) of proteins have brought about the accumulation of protein structures which completely lack functional information (Bentley et al., 2004; Murphy et al., 2004; Baxevanis, 2003; Miller et al., 2003). For instance, the Protein Data Bank (PDB), the world's repository for protein 3D structures, has recently witnessed an accumulation of experimentally determined protein 3D structures whose functions are unknown (Berman, H.M., & Westbrook, J.D. 2004). This, in turn, has created the need for computational methods of structure-based protein function prediction, especially those which can be implemented automatically in high-throughput fashion (Jung, J.W. & Lee, W. 2004; Yakunin, A.F., et al., 2004). One of the main roles of bioinformatics (or computational biology) in this post-genomic era of biology is to reduce the workload of the experimentalists by computationally "eliminating" candidates for experimentation, thereby allowing them to invest their time and effort on the "good" ones that are more likely to yield useful results. This is one of the main objectives of the present work.

There are a number of established ways to predict (computationally) the function of a protein whose 3D structure (and amino acid sequence) is known. One way to do this is to predict the ligand(s) that the protein binds. To do this based on the 3D structure of the protein, one can proceed by detecting the ligand's binding site - the ligand's specific 'signature' on its receptor protein - in the receptor protein's 3D structure. Ligands usually dock on the surface of a protein, and a ligand's binding site (BS, LBS) is "buried" within the receptor protein's interior to varying degrees.

The work we describe here involves the prediction of the binding sites of six biologically important ligands, namely: GTP, ATP, sialic acid, retinoic acid and nitric oxide in heme-bound and unbound forms. The biological roles of GTP and ATP are widely established (for example, see Mazzorana M, et al., 2008, and Stork P.J., 2003, respectively) Since both GTP- and ATP-binding proteins are highly heterogeneous, we focus here on the small Ras-type G-proteins (SRGP) and the ser/thr protein kinase (STPK) families, respectively. Sialic acid (SIA) is a C9 monosaccharide, and is the key component of mucus that allows the latter to prevent infections; more importantly, however, it has a significant role in the regulation of cellular communication (Lehmann et al., 2006; Miyagi et al., 2004). Retinoic acid (REA), on the other hand, has important roles in the transcriptional modulation of certain target genes by interacting with any one of its three known receptors: alpha, beta and gamma (Germain et al., 2006; Wolf, 2006). Finally, nitric oxide (NO) is an important signaling molecule in various cell types (Cary et al., 2006; Brunori et al., 2006; Perreti et al., 2006; Russwurm et al., 2004) which may either be in heme-bound (hNO) or unbound (fNO) forms.

The binding sites of these ligands were first characterized from ligand-containing experimentally solved structures from the PDB. This collection of structures from which the binding mode of the ligands are "learned" by an algorithm is called the 'training set' for the specific ligand in question. The salient features of the binding sites are then encoded in a tetrahedral tree data structure we designate as the '3D search motif' (3D SM). Using a novel analytical screening algorithm we developed earlier (Reyes, V.M., & Sheth, V.N., 2011; Reyes, V.M., 2015a), a set of some 801 experimentally solved but

functionally unannotated protein structures from the PDB were screened for these 3D search motifs. Of the 801, we detected 8 putative SRGP GTP-binding proteins, 61 putative STPK ATP-binding proteins, 35 putative SIA-binding proteins, 132 putative REA-binding proteins, 33 putative hNO-binding proteins, and 10 putative fNO-binding proteins. These candidate proteins were then subjected to the “cutting plane” and “tangent sphere” methods (Reyes, V.M., 2015b) as a further validation step. This method is a way to assess the degree of burial of a local functional site such as a ligand-binding site in a protein. The validation depends on the putative structure having the same or similar depth of ligand binding site burial as those in the training structures. To our knowledge, this work is the first computational investigation that predicts the binding sites for GTP, ATP, SIA, REA, hNO and fNO from among functionally unannotated structures in the PDB, and further screens those proteins using information regarding the depth of burial of the bound ligand within its cognate receptor protein.

2 Datasets and Methods.

2.1 The Training Structures.

The screening method used here has been reported previously by us (Reyes, V.M., & Sheth, V.N., 2011; Reyes, V.M., 2015a). It requires the construction of a ‘3D search motif’ (3D SM) from a set of training structures, and is based on the geometry and architecture of the ligand binding site (LBS) in question. The 3D SM is essentially a ‘signature’ of the LBS in question and contains at least six quantitative and eight qualitative parameters which are all inputted into the algorithm to enable it to detect the said LBS. The training structures for ATP-binding STPK proteins and GTP-binding SRGP proteins have been described and discussed in detail previously (ibid.). The training structures used for the construction of the 3D SM for the SIA are 1JSN, 1JSO, 1W0O, 1W0P, 1MQN (chains A and D); the training structures used to construct the 3D SM for REA are 1FM9, 1K74, 1FBY (chains A and B), 1FM6 (chains A and U), 1XDK (chains A and E), 1XLS (chains A, B, C and D), 2ACL (chains G, A, C and E); the training structures used for the construction of the 3D SM for hNO are 1OZW, 1XK3, 1ZOL (chains A and B); and finally, the training structures used to construct the 3D SM for fNO is 1ZGN, chains A and B. These training structures are all described in Table 1. The set of 801 protein structures in the PDB (all experimentally solved, mostly by x-ray crystallography) that lacked functional annotation at the time of this work are shown in Table 2. These proteins of unknown function come from many different species, but most are from *E. coli*, *T. maritima*, *T. thermophilus*, *B. subtilis*, *P. aeruginosa*, *H. influenzae* and *A. fulgidus*; only 18 (2.25%) come from *H. sapiens*. We used this set as the ‘application set’ – the set of 3D structures that we screened for the LBS’s in question for the purpose of assigning function to. In addition to determining the 3D SM from the above training structures, we also determined the depth of ligand burial in each, since this information is required in the next stages of our overall screening protocol.

2.2 Methods

2.2.1 Determination of the 3D SM’s.

The overall methodology followed in this work has been described in detail (Reyes, V.M., & Sheth, V.N., 2011; Reyes, V.M., 2015a). Briefly, the set of all hydrogen bonding (H-bonding) and van der Waals (VDW) interactions between ligand and protein in the training structures are sequestered (Engh, R.A. & Huber, R., 1991); Bondi, A., 1964). Then the most dominant and/or recurrent interactions among the training structures are determined, and designated the ‘3D binding consensus motif’. From such a consensus interaction mode between ligand and protein, the corresponding 3D SM is constructed. The 3D SM is a tetrahedral collection of four points in space representing the protein residues most commonly in association with the ligand (in the training structures). In the 3D SM, the

protein is in a reduced representation which we call the “double centroid reduced representation” (DCRR), where each amino acid is represented by two points, namely: the centroid of its backbone atoms (N, CA, C', O), and that of its side chain atoms (CB, CG, etc.). The application set is then screened for the tetrahedral 3D SM using a screening algorithm we developed earlier (ibid.). The tetrahedral 3D SM's for the six ligands in this study are shown in Figure 1, Panels A-D. The tetrahedral 3D SM is *not* just a collection of four points in space; it is a data structure that embodies a relatively large amount information about the binding site of the ligand in question. Specifically, it contains at least eight qualitative parameters, namely: the identities of the four amino acids in the tetrahedron (may be more if similar amino acids can interact with any of the ligand atoms in other receptor proteins) and their mode of association with the ligand (whether with backbone or side chain; hence, $4 \times 2 = 8$) and exactly six quantitative parameters (the lengths of the six sides of the tetrahedron) about the ligand binding site in question. Hence the 3D SM contains a total of $8 + 6 = 14$ combined qualitative and quantitative parameters. This property makes the algorithm optimally specific for the ligand in question (ibid.).

2.2.2 Determining the Degree of Burial of the Ligand Binding Sites.

In our screening protocol, there are two further steps after the detection of the LBS's using the 3D SM method (although this step is the most crucial). These two last steps depend on the “cutting plane” and “tangent sphere” methods (CPM and TSM, respectively) of ligand burial depth quantitative determination methods we reported previously (Reyes, V.M., 2015b; see also Figure 2). These two methods are complementary and produce numerical measures which we term the “CP index” (C_{Pi}) and “TS index” (T_{Si}), respectively, and which are essentially quantitative measures of the degrees of burial of a given ligand or LBS. These two additional steps are meant to narrow down the set of structures testing positive for the presence of a particular LBS and thus serve to further validate the prediction results. Specifically, those which have LBS burial depths resembling those in the training structures are deemed more likely to be true positives than those whose degrees of LBS burial are quite different.

3 Results

The determination of the 3D SM and the validation stage (testing positive and negative control structures) for the GTP-binding site in SRGPs and the ATP-binding site in STPKs have both been presented and discussed in detail in our previous work (Reyes, V.M., 2015a), so we shall not touch upon them here and just limit our discussion in the following sections to SIA, REA, hNO and fNO binding sites.

3.1 Determination of the 3D SM for Sialic Acid (SIA) Binding Sites.

The H-bonds between SIA and its receptor protein in the training structures are dominated by interactions between atom N5 of SIA and the backbone O of a Gly or a Val residue in the BS; atom O1A of SIA and either an NH1 atom of an Arg or an OE1 or NE2 atom of a Gln residue in the BS; and atom O8 of SIA and the hydroxyl O of a Ser or a Tyr residue in the BS. The VDW interactions, on the other hand, are mainly between atom C7 of SIA and either the CH2 side chain atom of a Trp or the CE side chain atom of a Met residue in the BS. Careful consideration of these interactions enabled us to build the 3D search motif for SIA shown in Figure 1A.

3.2 Determination of the 3D SM for Retinoic Acid (REA) Binding Sites.

The H-bonds between REA and its receptor protein in the training structures are dominated by interactions between atom O1 of REA and the terminal side chain amino group of an Arg residue, and atom O2 of REA and the backbone N of an Ala residue in the BS. The VDW interactions, on the other hand, are mainly between atom C3 of REA and one of the side chain carbon atoms of an Ile or a Val

residue in the BS; atom C17 of REA and either atom CB of a His or a Cys residue, or the backbone O of a Cys residue in the BS; and finally atom C20 of REA and the CD2 atom of a Phe or a Leu residue in the BS. Careful consideration of these interactions led us to construct the 3D SM for REA shown in Figure 1B.

3.3 Determination of the 3D SM for Heme-Bound Nitric Oxide (hNO) Binding Sites.

The H-bonds between hNO and its receptor protein in the training structures are dominated by interactions between the heme iron and the side chain amino group of a His residue in the BS; the O2D atom of heme and a side chain amino group of an Arg residue in the BS; and atom O of NO and a Gly residue atom or a side chain C atom of a Leu residue in the BS. The VDW interactions, on the other hand, are mainly between atom CHD of heme and a side chain C atom of a Phe or a Gly residue in the BS; and between atom O2D of heme and a side chain atom of a His or a Tyr residue in the BS. Careful consideration of the above interactions allowed us to build the 3D SM for hNO shown in Figure 1C.

3.4 Determination of the 3D SM for Free/Unbound Nitric Oxide (fNO) Binding Sites.

The H-bonds between fNO and its receptor protein in the single training structure (with two protein chains) involve N atom of fNO and the backbone N of an Arg residue or the side chain OH group of a Tyr residue in the BS. The VDW interactions, on the other hand, are mainly between the N atom of fNO and an atom of a Gly or a Val residue in the BS, or between atom O of fNO and a side chain C atom of an Ile or Phe residue in the BS. Careful consideration of these interactions allowed us to construct the 3D SM for unbound fNO shown in Figure 1D.

3.5 Validation Step: Positive and Negative Controls

3.5.1. Negative Control Structures.

Thirty negative control structures were used for the validation of the BS's for all six protein families studied here; they are, namely: 135L, 1A1M, 1A6T, 1BHC, 1PSN, 1BRF, 1EWK, 1CBN, 1MV5, 1JFF, 104M, 1ASH, 1B3B, 1BRF, 1CKO, 1CRP, 1EWK, 1F3O, 1FW5, 1HWY, 1JBP, 1MJJ, 1MV5, 1NQT, 1OGU, 1PE6, 1RDQ, 1SVS, 1TWY and 1Z3C. The above structures are all described in Table 3. Our results show that in all cases, the algorithm found no 3D SM in any of the negative control structures as expected. These results imply that the algorithm is highly specific for their respective ligands.

3.5.2. Positive Control Structures.

As for positive control structures, we note that there are no other appropriate positive structures in the PDB for the four above ligands as all of them have been used as training structures. Positive control structures to be used for validation must be yet "unseen" by the algorithm. We thus constructed artificial positive control structures from the negative control structures by replacing four appropriate amino acid residues in the latter to make a legitimate 3D SM for the particular ligand. These artificially mutated structures were then screened for the appropriate 3D SM using our algorithm. In all cases, the algorithm detected the artificially embedded 3D SM for the particular ligand (data not shown). These results imply that the screening algorithm has high sensitivity for the 3D SM corresponding to the particular ligand.

3.6 Screening Results

The screening process is illustrated in Figure 2. There are three stages in our screening process, the first stage and the most important being the LBS determination. The next stages involve the determination

of the LBS burial in the putative structures from the preceding stage. This is done by determining their CPi and TSi, respectively. The computed values are compared against the CPi and TSi of the respective training structures, and those putative structures having CPi and TSi closest to any of those of the training structures are deemed “double positives”, and are thus considered best ligand-binding candidates in their respective protein families (see below). The application set, the 801 functionally unannotated structures in the PDB that served as application structures for this study, is shown in Table 2. These proteins come from a diverse distribution of species (see Table 4). The ‘Cutting Plane’ and ‘Tangent Sphere’ methods, on the other hand, are illustrated in Figure 1, Panels A and B, of our previous paper (Reyes, V.M., 2015b), which schematically illustrate the two methods and how they complement each other.

Overall results are as follows: of the 801 application structures, we detected 61 putative ATP-binding STPK proteins (7.6%), eight GTP-binding SRGP proteins (1.0%), 35 putative SIA-binding proteins (4.4%), 132 putative REA-binding proteins (16.5%), 33 putative hNO binding proteins (4.1%), and 10 fNO binding proteins (1.2%). We now show the details of these screening results in the following sections. Note that a protein that tested positive for a particular LBS may have more than one chain, and one or more LBSs may have been detected in each chain.

In the first 6 subtables of Table 5, the blue entries on top are the training structures for the particular 3D SM. Meanwhile, the black entries below are the structures that tested positive for the ligand in question. The headings “CPM” and “TSM” stand for “cutting plane” and “tangent sphere” methods, respectively. The red arrows point out those positive structures whose CPM and TSM indices are either within an arbitrarily set difference, e.g., within 8-10%, from any one of those of the training structures, respectively, of the closest one in the set. In each case, integration of these ligand burial depth results with those of the LBS screening results further trim down the positive set, at the same time further validating the LBS existence prediction. The information contained in the different parts of the tables are illustrated and explained diagrammatically in part 7 (of 7) of Table 5. Note that due to the large number of structures testing positive for the LBS (first stage of screening) in question in the two cases of ATP-binding STPK and REA-binding protein families (Table 5, part 2 of 7 and part 4 of 7, respectively) this diagram is not strictly adhered to. Instead, only structures with CPi and TSi values within 10.0 Å of those of a training structure are shown.

3.6.1 Screening Results for GTP-Binding Sites in Small Ras-type G-Proteins. Eight structures (1.0% of the original 801) tested positive in the initial screening step, the detection of the 3D SM for GTP (Table 5, part 1 of 7). This set then got reduced to seven (0.9%) after matching their CPi or TSi (i.e., at least one of them) values to those of the training structures. From these seven structures, two (0.2%) stand out, namely, 1XT1 and 1RU8, because *both* of their CPi and TSi values are close to those of one of the structures in the training set (see Table 6).

3.6.2 Screening Results for ATP-Binding Sites in ser/thr Proein Kinases. The number of structures that tested positive for the ATP BS for this family is 61 (7.6%; see Table 5, part 2 of 7). By incorporating the ligand burial depth data from the CP and TS methods, 24 of the 61 structures testing positive for the ATP-binding site have been eliminated, leaving 37 structures (4.6%). Out of these 37, the following 11 to 13 structures (ca. 1.6%) are strong candidates because their CPi’s and TSi’s resemble both those of a training structure: 1WM6, 2CV1, 1RKQ, 1NF2, 1TQ6, 1MWW, 1TT7, 1T57, 1F19, 1RKI, 1Y9E (and possibly 1VPH and 1YYV as well; see Schwarzenbacher R. et al., 2004; Teplyakov A. et al., 2002; Beeby M. et al., 2005; Kunishima N. et al., 2005; see also Table 6).

3.6.3 Screening Results for Sialic Acid Binding Sites. For this ligand, 35 (4.4%) structures tested positive for the SIA binding site (Table 5, part 3 of 7). Of these, only 20 (2.5%) possess either a CPi or TSi close to that of a training structure. Of these 20, two structures (0.2%) namely, 1VKA and 1IUK, stand out as both of their CPi and TSi values resemble both the CPi and TSi values of one of the structures in the training set for this ligand (see Table 6).

3.6.4 Screening Results for Retinoic Acid Binding Sites. Of the 801 application structures, 132 (16.5%) tested positive for the REA binding site. Incorporating the ligand burial depth data from the CPM and TSM methods, almost 60% of the above 132 structures have been eliminated, leaving 53 candidate structures (6.6%; Table 5, part 4 of 7). The following 13 or 14 structures (ca. 1.7%) are strong candidates because both their CPi's and TSi's resemble both those of a training structure: 1Y8T, 1Y8U, 1Y8V, 1Y8W, 1Y8X, 1Y8Y, 1Y8Z, 1Y9A, 1Y9B, 1Y9C, 1Y9D, 1Y9E, 1Y9F, 1Y9G, 1Y9H, 1Y9I, 1Y9J, 1Y9K, 1Y9L, 1Y9M, 1Y9N, 1Y9O, 1Y9P, 1Y9Q, 1Y9R, 1Y9S, 1Y9T, 1Y9U, 1Y9V, 1Y9W, 1Y9X, 1Y9Y, 1Y9Z, 1Y9AA, 1Y9AB, 1Y9AC, 1Y9AD, 1Y9AE, 1Y9AF, 1Y9AG, 1Y9AH, 1Y9AI, 1Y9AJ, 1Y9AK, 1Y9AL, 1Y9AM, 1Y9AN, 1Y9AO, 1Y9AP, 1Y9AQ, 1Y9AR, 1Y9AS, 1Y9AT, 1Y9AU, 1Y9AV, 1Y9AW, 1Y9AX, 1Y9AY, 1Y9AZ, 1Y9BA, 1Y9BB, 1Y9BC, 1Y9BD, 1Y9BE, 1Y9BF, 1Y9BG, 1Y9BH, 1Y9BI, 1Y9BJ, 1Y9BK, 1Y9BL, 1Y9BM, 1Y9BN, 1Y9BO, 1Y9BP, 1Y9BQ, 1Y9BR, 1Y9BS, 1Y9BT, 1Y9BU, 1Y9BV, 1Y9BW, 1Y9BX, 1Y9BY, 1Y9BZ, 1Y9CA, 1Y9CB, 1Y9CC, 1Y9CD, 1Y9CE, 1Y9CF, 1Y9CG, 1Y9CH, 1Y9CI, 1Y9CJ, 1Y9CK, 1Y9CL, 1Y9CM, 1Y9CN, 1Y9CO, 1Y9CP, 1Y9CQ, 1Y9CR, 1Y9CS, 1Y9CT, 1Y9CU, 1Y9CV, 1Y9CW, 1Y9CX, 1Y9CY, 1Y9CZ, 1Y9DA, 1Y9DB, 1Y9DC, 1Y9DD, 1Y9DE, 1Y9DF, 1Y9DG, 1Y9DH, 1Y9DI, 1Y9DJ, 1Y9DK, 1Y9DL, 1Y9DM, 1Y9DN, 1Y9DO, 1Y9DP, 1Y9DQ, 1Y9DR, 1Y9DS, 1Y9DT, 1Y9DU, 1Y9DV, 1Y9DW, 1Y9DX, 1Y9DY, 1Y9DZ, 1Y9EA, 1Y9EB, 1Y9EC, 1Y9ED, 1Y9EE, 1Y9EF, 1Y9EG, 1Y9EH, 1Y9EI, 1Y9EJ, 1Y9EK, 1Y9EL, 1Y9EM, 1Y9EN, 1Y9EO, 1Y9EP, 1Y9EQ, 1Y9ER, 1Y9ES, 1Y9ET, 1Y9EU, 1Y9EV, 1Y9EW, 1Y9EX, 1Y9EY, 1Y9EZ, 1Y9FA, 1Y9FB, 1Y9FC, 1Y9FD, 1Y9FE, 1Y9FF, 1Y9FG, 1Y9FH, 1Y9FI, 1Y9FJ, 1Y9FK, 1Y9FL, 1Y9FM, 1Y9FN, 1Y9FO, 1Y9FP, 1Y9FQ, 1Y9FR, 1Y9FS, 1Y9FT, 1Y9FU, 1Y9FV, 1Y9FW, 1Y9FX, 1Y9FY, 1Y9FZ, 1Y9GA, 1Y9GB, 1Y9GC, 1Y9GD, 1Y9GE, 1Y9GF, 1Y9GG, 1Y9GH, 1Y9GI, 1Y9GJ, 1Y9GK, 1Y9GL, 1Y9GM, 1Y9GN, 1Y9GO, 1Y9GP, 1Y9GQ, 1Y9GR, 1Y9GS, 1Y9GT, 1Y9GU, 1Y9GV, 1Y9GW, 1Y9GX, 1Y9GY, 1Y9GZ, 1Y9HA, 1Y9HB, 1Y9HC, 1Y9HD, 1Y9HE, 1Y9HF, 1Y9HG, 1Y9HH, 1Y9HI, 1Y9HJ, 1Y9HK, 1Y9HL, 1Y9HM, 1Y9HN, 1Y9HO, 1Y9HP, 1Y9HQ, 1Y9HR, 1Y9HS, 1Y9HT, 1Y9HU, 1Y9HV, 1Y9HW, 1Y9HX, 1Y9HY, 1Y9HZ, 1Y9IA, 1Y9IB, 1Y9IC, 1Y9ID, 1Y9IE, 1Y9IF, 1Y9IG, 1Y9IH, 1Y9II, 1Y9IJ, 1Y9IK, 1Y9IL, 1Y9IM, 1Y9IN, 1Y9IO, 1Y9IP, 1Y9IQ, 1Y9IR, 1Y9IS, 1Y9IT, 1Y9IU, 1Y9IV, 1Y9IW, 1Y9IX, 1Y9IY, 1Y9IZ, 1Y9JA, 1Y9JB, 1Y9JC, 1Y9JD, 1Y9JE, 1Y9JF, 1Y9JG, 1Y9JH, 1Y9JI, 1Y9JJ, 1Y9JK, 1Y9JL, 1Y9JM, 1Y9JN, 1Y9JO, 1Y9JP, 1Y9JQ, 1Y9JR, 1Y9JS, 1Y9JT, 1Y9JU, 1Y9JV, 1Y9JW, 1Y9JX, 1Y9JY, 1Y9JZ, 1Y9KA, 1Y9KB, 1Y9KC, 1Y9KD, 1Y9KE, 1Y9KF, 1Y9KG, 1Y9KH, 1Y9KI, 1Y9KJ, 1Y9KK, 1Y9KL, 1Y9KM, 1Y9KN, 1Y9KO, 1Y9KP, 1Y9KQ, 1Y9KR, 1Y9KS, 1Y9KT, 1Y9KU, 1Y9KV, 1Y9KW, 1Y9KX, 1Y9KY, 1Y9KZ, 1Y9LA, 1Y9LB, 1Y9LC, 1Y9LD, 1Y9LE, 1Y9LF, 1Y9LG, 1Y9LH, 1Y9LI, 1Y9LJ, 1Y9LK, 1Y9LL, 1Y9LM, 1Y9LN, 1Y9LO, 1Y9LP, 1Y9LQ, 1Y9LR, 1Y9LS, 1Y9LT, 1Y9LU, 1Y9LV, 1Y9LW, 1Y9LX, 1Y9LY, 1Y9LZ, 1Y9MA, 1Y9MB, 1Y9MC, 1Y9MD, 1Y9ME, 1Y9MF, 1Y9MG, 1Y9MH, 1Y9MI, 1Y9MJ, 1Y9MK, 1Y9ML, 1Y9MN, 1Y9MO, 1Y9MP, 1Y9MQ, 1Y9MR, 1Y9MS, 1Y9MT, 1Y9MU, 1Y9MV, 1Y9MW, 1Y9MX, 1Y9MY, 1Y9MZ, 1Y9NA, 1Y9NB, 1Y9NC, 1Y9ND, 1Y9NE, 1Y9NF, 1Y9NG, 1Y9NH, 1Y9NI, 1Y9NJ, 1Y9NK, 1Y9NL, 1Y9NM, 1Y9NN, 1Y9NO, 1Y9NP, 1Y9NQ, 1Y9NR, 1Y9NS, 1Y9NT, 1Y9NU, 1Y9NV, 1Y9NW, 1Y9NX, 1Y9NY, 1Y9NZ, 1Y9OA, 1Y9OB, 1Y9OC, 1Y9OD, 1Y9OE, 1Y9OF, 1Y9OG, 1Y9OH, 1Y9OI, 1Y9OJ, 1Y9OK, 1Y9OL, 1Y9OM, 1Y9ON, 1Y9OO, 1Y9OP, 1Y9OQ, 1Y9OR, 1Y9OS, 1Y9OT, 1Y9OU, 1Y9OV, 1Y9OW, 1Y9OX, 1Y9OY, 1Y9OZ, 1Y9PA, 1Y9PB, 1Y9PC, 1Y9PD, 1Y9PE, 1Y9PF, 1Y9PG, 1Y9PH, 1Y9PI, 1Y9PJ, 1Y9PK, 1Y9PL, 1Y9PM, 1Y9PN, 1Y9PO, 1Y9PP, 1Y9PQ, 1Y9PR, 1Y9PS, 1Y9PT, 1Y9PU, 1Y9PV, 1Y9PW, 1Y9PX, 1Y9PY, 1Y9PZ, 1Y9QA, 1Y9QB, 1Y9QC, 1Y9QD, 1Y9QE, 1Y9QF, 1Y9QG, 1Y9QH, 1Y9QI, 1Y9QJ, 1Y9QK, 1Y9QL, 1Y9QM, 1Y9QN, 1Y9QO, 1Y9QP, 1Y9QQ, 1Y9QR, 1Y9QS, 1Y9QT, 1Y9QU, 1Y9QV, 1Y9QW, 1Y9QX, 1Y9QY, 1Y9QZ, 1Y9RA, 1Y9RB, 1Y9RC, 1Y9RD, 1Y9RE, 1Y9RF, 1Y9RG, 1Y9RH, 1Y9RI, 1Y9RJ, 1Y9RK, 1Y9RL, 1Y9RM, 1Y9RN, 1Y9RO, 1Y9RP, 1Y9RQ, 1Y9RR, 1Y9RS, 1Y9RT, 1Y9RU, 1Y9RV, 1Y9RW, 1Y9RX, 1Y9RY, 1Y9RZ, 1Y9SA, 1Y9SB, 1Y9SC, 1Y9SD, 1Y9SE, 1Y9SF, 1Y9SG, 1Y9SH, 1Y9SI, 1Y9SJ, 1Y9SK, 1Y9SL, 1Y9SM, 1Y9SN, 1Y9SO, 1Y9SP, 1Y9SQ, 1Y9SR, 1Y9SS, 1Y9ST, 1Y9SU, 1Y9SV, 1Y9SW, 1Y9SX, 1Y9SY, 1Y9SZ, 1Y9TA, 1Y9TB, 1Y9TC, 1Y9TD, 1Y9TE, 1Y9TF, 1Y9TG, 1Y9TH, 1Y9TI, 1Y9TJ, 1Y9TK, 1Y9TL, 1Y9TM, 1Y9TN, 1Y9TO, 1Y9TP, 1Y9TQ, 1Y9TR, 1Y9TS, 1Y9TT, 1Y9TU, 1Y9TV, 1Y9TW, 1Y9TX, 1Y9TY, 1Y9TZ, 1Y9UA, 1Y9UB, 1Y9UC, 1Y9UD, 1Y9UE, 1Y9UF, 1Y9UG, 1Y9UH, 1Y9UI, 1Y9UJ, 1Y9UK, 1Y9UL, 1Y9UM, 1Y9UN, 1Y9UO, 1Y9UP, 1Y9UQ, 1Y9UR, 1Y9US, 1Y9UT, 1Y9UU, 1Y9UV, 1Y9UW, 1Y9UX, 1Y9UY, 1Y9UZ, 1Y9VA, 1Y9VB, 1Y9VC, 1Y9VD, 1Y9VE, 1Y9VF, 1Y9VG, 1Y9VH, 1Y9VI, 1Y9VJ, 1Y9VK, 1Y9VL, 1Y9VM, 1Y9VN, 1Y9VO, 1Y9VP, 1Y9VQ, 1Y9VR, 1Y9VS, 1Y9VT, 1Y9VU, 1Y9VV, 1Y9VW, 1Y9VX, 1Y9VY, 1Y9VZ, 1Y9WA, 1Y9WB, 1Y9WC, 1Y9WD, 1Y9WE, 1Y9WF, 1Y9WG, 1Y9WH, 1Y9WI, 1Y9WJ, 1Y9WK, 1Y9WL, 1Y9WM, 1Y9WN, 1Y9WO, 1Y9WP, 1Y9WQ, 1Y9WR, 1Y9WS, 1Y9WT, 1Y9WU, 1Y9WV, 1Y9WW, 1Y9WX, 1Y9WY, 1Y9WZ, 1Y9XA, 1Y9XB, 1Y9XC, 1Y9XD, 1Y9XE, 1Y9XF, 1Y9XG, 1Y9XH, 1Y9XI, 1Y9XJ, 1Y9XK, 1Y9XL, 1Y9XM, 1Y9XN, 1Y9XO, 1Y9XP, 1Y9XQ, 1Y9XR, 1Y9XS, 1Y9XT, 1Y9XU, 1Y9XV, 1Y9XW, 1Y9XX, 1Y9XY, 1Y9XZ, 1Y9YA, 1Y9YB, 1Y9YC, 1Y9YD, 1Y9YE, 1Y9YF, 1Y9YG, 1Y9YH, 1Y9YI, 1Y9YJ, 1Y9YK, 1Y9YL, 1Y9YM, 1Y9YN, 1Y9YO, 1Y9YP, 1Y9YQ, 1Y9YR, 1Y9YS, 1Y9YT, 1Y9YU, 1Y9YV, 1Y9YW, 1Y9YX, 1Y9YY, 1Y9YZ, 1Y9ZA, 1Y9ZB, 1Y9ZC, 1Y9ZD, 1Y9ZE, 1Y9ZG, 1Y9ZH, 1Y9ZI, 1Y9ZJ, 1Y9ZK, 1Y9ZL, 1Y9ZM, 1Y9ZN, 1Y9ZO, 1Y9ZP, 1Y9ZQ, 1Y9ZR, 1Y9ZS, 1Y9ZT, 1Y9ZU, 1Y9ZV, 1Y9ZW, 1Y9ZX, 1Y9ZY, 1Y9ZZ, 1Z6M, and 1VIM (and possibly 1ZE0 as well; see Clifton, I.J. et al., 2003; Asch WS, Schechter N., 2000; see also Table 6).

3.6.5 Screening for Heme-Bound NO Binding Sites. For this ligand, 33 structures (4.1%) tested positive for the hNO binding site. They have been further trimmed down to 12 (1.5%) upon incorporation of the ligand burial data using the CPM and TSM (Table 5, part 5 of 7). Of these 12, four structures (0.5%), namely 1ZSW, 1VKH, 1UAN and 2B4W stand out as their CPi and TSi values resemble both those from a training structure for this ligand (see Arndt, J.W. et al. 2005; Zhou C.Z. et al., 2005; see also Table 6).

3.6.6 Screening for Free/Unbound NO Binding Sites. In this set, the 10 structures (1.2%) tested positive for the fNO binding site. These have been narrowed down to six (0.7%) upon including the results from the CPM and TSM ligand burial data (Table 5, part 6 of 7). Of these six, a single structure (0.1%), namely, 1UC2, stands out as its CPi and TSi values both resemble those by the lone training structure, 1ZGN., for this ligand (see Table 6).

4 Discussion.

Using a novel analytical screening algorithm we developed earlier (Reyes, V.M., & Sheth, V.N., 2011; Reyes, V.M., 2015a), we have screened some 801 functionally unannotated x-ray diffraction structures deposited in the PDB for the binding sites of GTP, ATP, sialic acid, retinoic acid, and heme-bound and unbound nitric oxide. We detected eight SRGP GTP-binding sites, 61 STPK ATP-binding sites, 35 SIA-binding sites, 132 REA-binding sites, 33 hNO-binding sites and 10 fNO binding sites, with some structures containing more than one binding site for the ligand in question. The detection of the LBS for a particular ligand was accomplished by detecting the 3D SM for that ligand in the protein structures. This idea depends on the assumption that the 3D SM (and hence the binding site characteristics) for a given ligand is conserved within a protein family.

Using another novel analytical method we developed earlier (Reyes, V.M., 2015b) called the “cutting plane” and “tangent sphere” methods, the degrees of burial of these ligand binding sites were also determined and used as a further validation step for the ligand binding prediction. Thus the positive structures above were further culled by comparing their CPi or TSi to those of the training structures for the protein family and those which had similar values were retained, the rationale being those which have depths of LBS burial resembling those in the training structures are deemed more likely to be true positives than those who do not. This criterion depends on the reasonable premise that ligand burial depth is characteristic of a particular ligand-binding protein family.

Our LBS detection method depends on the availability of protein complex 3D structures with the bound ligand under study and as such relies heavily on the contents of the PDB. Although experimental structures for GTP- and ATP-binding proteins abound in the PDB, structures of proteins bound with other ligands are underrepresented. For example, the scarcity of structures containing SIA, REA, hNO and fNO in the PDB is a limitation in terms of having an ample number of both training and control (validation) sets for our screening algorithm. However, since our screening algorithm is largely analytical, the need for exhaustive positive and negative control structures is not that critical compared to statistical algorithms such as those based on SVM and neural networks. This is one advantage of an analytical algorithm over a stochastic one.

The fuzzy factor or margin, ϵ , we incorporate into the branches and node-edges in the 3D SM are usually in the order of 1.0 - 1.5 Å (Reyes, V.M. & Sheth, V.N., 2011; Reyes, V.M., 2015a). Thus in

cases where the protein assumes drastic conformational changes upon ligand binding and displacements of amino acid residues at the binding site are much greater than 1.5 Å, our method will perhaps likely fail. We believe it is reasonable to assume that the deeper within the protein interior the LBS lies, the more drastic the conformational changes the protein undergoes upon binding the ligand (i.e., in transitioning from the ‘apo’ to the complexed form). But whether or not the predictive power of our algorithm decreases as the LBS lies deeper within the protein remains to be investigated.

In the determination of H-bonds between protein and ligand to build the 3D SM, we did not ascertain the linearity of the bonds of the interacting atoms between ligand and protein (amino acids in the BS); we merely measured non-hydrogen interatomic distances and we sequester only those with perfect or near-perfect H-bond distances (2.7Å-2.9 Å). Thus this issue is unlikely to have a significant adverse effect on our results, as instances in which the H-bonding atoms have perfect or near-perfect H-bonding distances and at the same time non-linear, are quite rare.

5 Summary and Conclusions.

By determining the most prevalent and/or dominant H-bonding and VDW interactions between ligand atoms and amino acid residue atoms in the BS of its receptor protein, we have constructed a ‘signature’ of the binding sites of six biologically important ligands – GTP, ATP, SIA, REA, hNO and fNO. We designate this ‘signature’ as the 3D BS consensus motif for the particular ligand. We have then encoded these binding site signatures in a tetrahedral tree data structure we call the 3D search motif or “3D SM” for the ligand in question. Then, using a novel analytical search algorithm we developed earlier (Reyes, V.M., & Sheth, V.N., 2011; Reyes, V.M., 2015a) experimentally determined protein structures in the PDB that lacked functional annotation were screened for the above five ligands. We detected eight structures with the GTP-binding site of the SRGP family, 61 structures with the ATP-binding site of the STPK family, 35 structures with the SIA binding site signature, 132 with the REA's, 33 with the heme-bound NO's, and 10 with the free NO's. The positive proteins above were further subjected to validation by determining the depth of burial of their LBS's using their CPi and TSi values and comparing them to those of their training structures. Respectively seven, 37, 20, 53, 12, and six of the GTP-, ATP-, SIA-, REA-, hNO- and fNO-binding proteins had *either* their CPi *or* TSi close to those of a retaining structure for the protein family. Of these, respectively two, 28 (of which 13 stand out from the rest), two, 30 (of which 14 stand out from the rest), four and one of the GTP-, ATP-, SIA-, REA-, hNO- and fNO-binding proteins had *both* of their CPi *and* TSi close to those of a retaining structure for the protein family. Thus by incorporating information about the depth of LBS burial in the positive proteins from the 3D SM screening, they can be further narrowed down significantly for increased confidence in the LBS prediction. At this point in the protein function prediction process, the job of the bioinformaticist is usually done and the experimentalists take over. Thus we are currently awaiting experimental verification of the results we report here. Our final results are shown in Table 6.

Acknowledgments. This work was supported by an Institutional Research and Academic Career Development Award to the author, NIGMS/NIH grant number GM 68524. The author also wishes to acknowledge the San Diego Supercomputer Center, the UCSD Academic Computing Services, and the UCSD Biomedical Library, for the help and support of their staff and personnel. He also acknowledges the Division of Research Computing at RIT, and computing resources from the Dept. of Biological Sciences, College of Science, at RIT.

References

Arndt JW, Schwarzenbacher R, Page R, Abdubek P, Ambing E, Biorac T, Canaves JM, Chiu HJ, Dai X, Deacon AM, DiDonato M, Elsliger MA, Godzik A, Grittini C, Grzechnik SK, Hale J, Hampton E,

Han GW, Haugen J, Hornsby M, Klock HE, Koesema E, Kreusch A, Kuhn P, Jaroszewski L, Lesley SA, Levin I, McMullan D, McPhillips TM, Miller MD, Morse A, Moy K, Nigoghossian E, Ouyang J, Peti WS, Quijano K, Reyes R, Sims E, Spraggon G, Stevens RC, van den Bedem H, Velasquez J, Vincent J, von Delft F, Wang X, West B, White A, Wolf G, Xu Q, Zagnitko O, Hodgson KO, Wooley J, Wilson IA. "Crystal structure of an alpha/beta serine hydrolase (YDR428C) from *Saccharomyces cerevisiae* at 1.85 Å resolution." *Proteins*. 2005 Feb 15;58(3):755-8.

Asch WS, Schechter N. "Plasticin, a type III neuronal intermediate filament protein, assembles as an obligate heteropolymer: implications for axonal flexibility." *J Neurochem*. 2000 Oct;75(4):1475-86.

Baxevis, A.D. 2003. Using genomic databases for sequence-based biological discovery. *Mol Med*. 9:185-92.

Beeby M, O'Connor BD, Ryttersgaard C, Boutz DR, Perry LJ, Yeates TO. "The genomics of disulfide bonding and protein stabilization in thermophiles." *PLoS Biol*. 2005 Sep;3(9):e309. Epub 2005 Aug 23.

Bentley, S.D., and Parkhill, J. 2004. Comparative genomic structure of prokaryotes. *Annu Rev Genet*. 38:771-92.

Berman, H.M., and Westbrook, J.D. 2004. The impact of structural genomics on the protein data bank. *Am J Pharmacogenomics*. 4:247-52.

Bondi, A, 1964, "Van der Waals Volumes and Radii", *J. Phys. Chem.*, **68**(3):441-451

Brunori M, Forte E, Arese M, Mastronicola D, Giuffrè A, Sarti P. "Nitric oxide and the respiratory enzyme." *Biochim Biophys Acta*. 2006 Sep-Oct;1757(9-10):1144-54. Epub 2006 May 13.

Burley, S.K. 2000. An overview of structural genomics. *Nat Struct Biol*. 7 Suppl:932-4.

Cary SP, Winger JA, Derbyshire ER, Marletta MA. "Nitric oxide signaling: no longer simply on or off." *Trends Biochem Sci*. 2006 Apr;31(4):231-9. Epub 2006 Mar 10.

Clifton IJ, Doan LX, Sleeman MC, Topf M, Suzuki H, Wilmouth RC, Schofield CJ. "Crystal structure of carbapenem synthase (CarC)." *J Biol Chem*. 2003 Jun 6;278(23):20843-50. Epub 2003 Feb 28.

Engh, R.A. & Huber, R. (1991) Accurate bond and angle parameters for X-ray protein structure refinement. *Acta Cryst*. (1991). A47, 392-400

Germain P, Chambon P, Eichele G, Evans RM, Lazar MA, Leid M, De Lera AR, Lotan R, Mangelsdorf DJ, Gronemeyer H. "International Union of Pharmacology. LX. Retinoic acid receptors." *Pharmacol Rev*. 2006 Dec;58(4):712-25.

Heinemann, U. 2000. Structural genomics in Europe: slow start, strong finish? *Nat Struct Biol*. 7 Suppl:940-2.

Jung, J.W., and Lee, W. 2004. Structure-based functional discovery of proteins: structural proteomics. *J Biochem Mol Biol*. 37:28-34.

Kunishima N, Asada Y, Sugahara M, Ishijima J, Nodake Y, Sugahara M, Miyano M, Kuramitsu S, Yokoyama S, Sugahara M. "A novel induced-fit reaction mechanism of asymmetric hot dog thioesterase PAAI." *J Mol Biol*. 2005 Sep 9;352(1):212-28.

Lehmann F, Tiralongo E, Tiralongo J. "Sialic acid-specific lectins: occurrence, specificity and function." *Cell Mol Life Sci*. 2006 Jun;63(12):1331-54.

Mazzorana M, Pinna LA, Battistutta R. "A structural insight into CK2 inhibition." *Mol Cell Biochem*. 2008 Sep;316(1-2):57-62.

- Miller, W., Makova, K.D., Nekrutenko, A., and Hardison, R.C. 2004. Comparative genomics. *Annu Rev Genomics Hum Genet.* 5:15-56.
- Miyagi T, Wada T, Yamaguchi K, Hata K. "Sialidase and malignancy: a minireview." *Glycoconj J.* 2004;20(3):189-98.
- Murphy, W.J., Pevzner, P.A., and O'Brien, S.J. 2004. Mammalian phylogenomics comes of age. *Trends Genet.* 20:631-9.
- Norrvell, J.C., and Machalek, A.Z. 2000. Structural genomics programs at the US National Institute of General Medical Sciences. *Nat Struct Biol.* 7 Suppl:931.
- Perretti M, D'Acquisto F. "Novel aspects of annexin 1 and glucocorticoid biology: intersection with nitric oxide and the lipoxin receptor." *Inflamm Allergy Drug Targets.* 2006 Apr;5(2):107-14.
- Reyes, V.M. & Sheth, V.N., "Visualization of Protein 3D Structures in 'Double-Centroid' Reduced Representation: Application to Ligand Binding Site Modeling and Screening", 2011, Handbook of Research in Computational and Systems Biology: Interdisciplinary Approaches, IGI-Global/Springer, pp. 583-598.
- Reyes, V.M. (2015a) "An Automatable Analytical Algorithm for Structure-Based Protein Functional Annotation via Detection of Specific Ligand 3D Binding Sites: Application to ATP Binding Sites in ser/thr Protein Kinases and GTP Binding Sites in Small Ras-type G-Proteins" (forthcoming; submitted to www.arXiv.org on Jan. 17, 2015); Abstract: Reyes, V.M., "Pharmacophore Modeling Using a Reduced Protein Representation as a Tool for Structure-Based Protein Function Prediction", *J. Biomol. Struct. & Dyn.*, Book of Abstracts, Albany 2009: The 16th Conversation, June 16-20, 2009, Vol. 26 (6) June 2009, p. 873
- Reyes, V.M. (2015b) "Two Complementary Methods for Relative Quantification of Ligand Binding Site Burial Depth in Proteins: The 'Cutting Plane' and 'Tangent Sphere' Methods" (forthcoming; submitted to www.arXiv.org on Feb. 5, 2015); Abstract: Cheguri, S. and Reyes, V.M., "A Database/Webserver for Size-Independent Quantification of Ligand Binding Site Burial Depth in Receptor Proteins: Implications on Protein Dynamics", *J. Biomol. Struct. & Dyn.*, Book of Abstracts, Albany 2011: The 17th Conversation, June 14-18, 2011, Vol. 28 (6) June 2011, p. 1013
- Russwurm M, Koesling D. "NO activation of guanylyl cyclase." *EMBO J.* 2004 Nov 10; 23(22):4443-50. Epub 2004 Oct 28.
- Schwarzenbacher R, Deacon AM, Jaroszewski L, Brinen LS, Canaves JM, Dai X, Elsliger MA, Floyd R, Godzik A, Grittini C, Grzechnik SK, Klock HE, Koesema E, Kovarik JS, Kreuzsch A, Kuhn P, Lesley SA, McMullan D, McPhillips TM, Miller MD, Morse A, Moy K, Nelson MS, Ouyang J, Page R, Robb A, Quijano K, Spraggon G, Stevens RC, van den Bedem H, Velasquez J, Vincent J, von Delft F, Wang X, West B, "Crystal structure of a putative glutamine amido transferase (TM1158) from *Thermotoga maritima* at 1.7 Å resolution." *Proteins.* 2004 Mar 1;54(4):801-5.
- Stork PJ. "Does Rap1 deserve a bad Rap?" *Trends Biochem Sci.* 2003 May;28(5):267-75.
- Tepljakov A, Obmolova G, Tordova M, Thanki N, Bonander N, Eisenstein E, Howard AJ, Gilliland GL. "Crystal structure of the YjeE protein from *Haemophilus influenzae*: a putative ATPase involved in cell wall synthesis." *Proteins.* 2002 Aug 1;48(2):220-6.
- Terwilliger, T.C. 2000. Structural genomics in North America. *Nat Struct Biol.* 7 Suppl:935-9.
- Wolf G "Is 9-cis-retinoic acid the endogenous ligand for the retinoic acid-X receptor?" *Nutr Rev.* 2006 Dec;64(12):532-8.
- Yakunin, A.F., Yee A.A., Savchenko, A., Edwards, A.M., and Arrowsmith, C.H. 2004. Structural proteomics: a tool for genome annotation. *Curr Opin Chem Biol.* 8:42-8.

Zhou CZ, Meyer P, Quevillon-Cheruel S, De La Sierra-Gallay IL, Collinet B, Graille M, Blondeau K, François JM, Leulliot N, Sorel I, Poupon A, Janin J, Van Tilbeurgh H. "Crystal structure of the YML079w protein from *Saccharomyces cerevisiae* reveals a new sequence family of the jelly-roll fold." *Protein Sci.* 2005 Jan;14(1):209-15.

FIGURE LEGENDS:

Figure 1, Panels A-D: The 3D Search Motifs. The 3D search motifs for the four ligands under study are shown: Panels A-D: Sialic acid, retinoic acid, heme-bound nitric oxide, and unbound nitric oxide search motifs, respectively. The lengths of the six sides of the tetrahedral motif (in Å) are also shown in an accompanying side table; the numbers inside parentheses are the corresponding standard deviations from the training structures. The ligand in each case is shown with its component atom names. The amino acids representing the tetrahedral vertices are indicated, with "(s)" indicating side chain interaction with ligand, and "(b)", backbone interaction. The root and three nodes are also indicated by the boxed letters.

Figure 2. The Elimination Process. Both local and global structure information are utilized in the process of elimination to search for candidate positive structures. Set A, the outermost red circle, represents the starting test/application set composed of 801 PDB structures without functional annotation. They are first screened for the particular 3D SM in question, and those that test positive, i.e., those that possess the 3D SM, form a subset of A; we call it set B (blue circle). Set B structures are then subjected to the "Cutting Plane" and "Tangent sphere" Methods (Reyes, V.M., 2015b). The CPM and TSM indices (CPMi and TSMi, respectively) of each structure are then compared respectively to those of the training structures used to create the 3D SM's. Those whose CPMi or TSMi are within several units (typically 8-10) of those of the training structures, are considered to have similar indices, and form a subset of B; we call it set C (brown circle). Structures in set C are further analyzed to determine whether their indices are both respectively similar to those any one or more of the training structures. Those which satisfy this criterion form a subset of C, which we call set D (green circle). This main advantage of this elimination procedure is it can be automated and ran in batch or high-throughput mode, without the requirement for human intervention, a feature desired of analytical tools for large datasets.

TABLE LEGENDS:

Table 1. The Training Sets. The training structures for the determination of the 3D SMs for the binding sites of sialic acid, retinoic, and heme-bound and unbound nitric oxide, are shown. The PDB IDs of the structures are shown on column 1, the source organism on column 2, and a brief description of the structures is on column 3.

Table 2. The Control Structures. Negative control structures for SA, RA, hNO and fNO binding sites are shown. As for positive control structures for those ligand binding sites, please see text. Positive and negative control structures used for validating the 3D SM's for GTP-binding SRGP and ATP-binding STPK protein families are taken up in detail in our previous work (Reyes, V.M., 2015a).

Table 3. The 801 Functionally Unannotated Proteins in the PDB Used As Application Structures. These 801 structures were obtained from the PDB in early 2006 by querying the PDB search site with the words "unknown function" or similar phrase. The absence of functional annotation in all 801 structures was further confirmed by examining the header information in each PDB file, which contained the phrase "function unknown" or a similar one in each case.

Table 4. Species Distribution of Application Set. The species distribution of the 801 application structures is shown in this table. The 801 structures come from 104 known species (that include bacteria, archaea, protozoans, and some higher organisms including humans), an uncultured bacterium (unknown species), and one is a synthetic protein. The 5 most represented species are *E. coli* (11.0%), *T. maritima* (7.9%), *T. thermophilus* (7.0%), *B. subtilis* (6.0%) and *P. aeruginosa* (4.7%).

Table 5, Parts 1-7. Cutting Plane and Tangent Sphere Indices Used to Assess LBS Burial in Screening Results: GTP in Small Ras-type GP (part 1 of 7); ATP in ser/thr PK; (part 2 of 7); Sialic Acid (part 3 of 7); Retinoic Acid (part 4 of 7); Heme-Bound NO (part 5 of 7); Unbound NO (part 6 of 7). The information in the above six tables is illustrated and identified schematically in part 7 of 7 of the table. Results of the determination of the particular binding site burial using the “cutting plane” and tangent sphere” methods are shown (headings “CPM” and “TSM”, respectively). The degree of burial is expressed as % of protein atoms on the exterior side of the cutting plane and inside the tangent sphere, respectively. Part 7 of 7 diagrammatically identifies what information are contained in the tables above based on their location in the table.

Table 6. Application Structures that Tested Positive. The structures from the set of 801 functionally unannotated proteins (Table 3) in the PDB that tested positive of the 3D SMs of GTP (in small, Ras-type G-proteins, ATP (in ser/thr protein kinases), sialic acid, retinoic acid, and heme-bound and unbound nitric oxide are summarized in this table. Note that most of the structures are still functionally unannotated at the time of this writing, as shown by the scarcity of entries in the last column, which is the published reference papers for the particular structure (see also References section).

FIGURES:

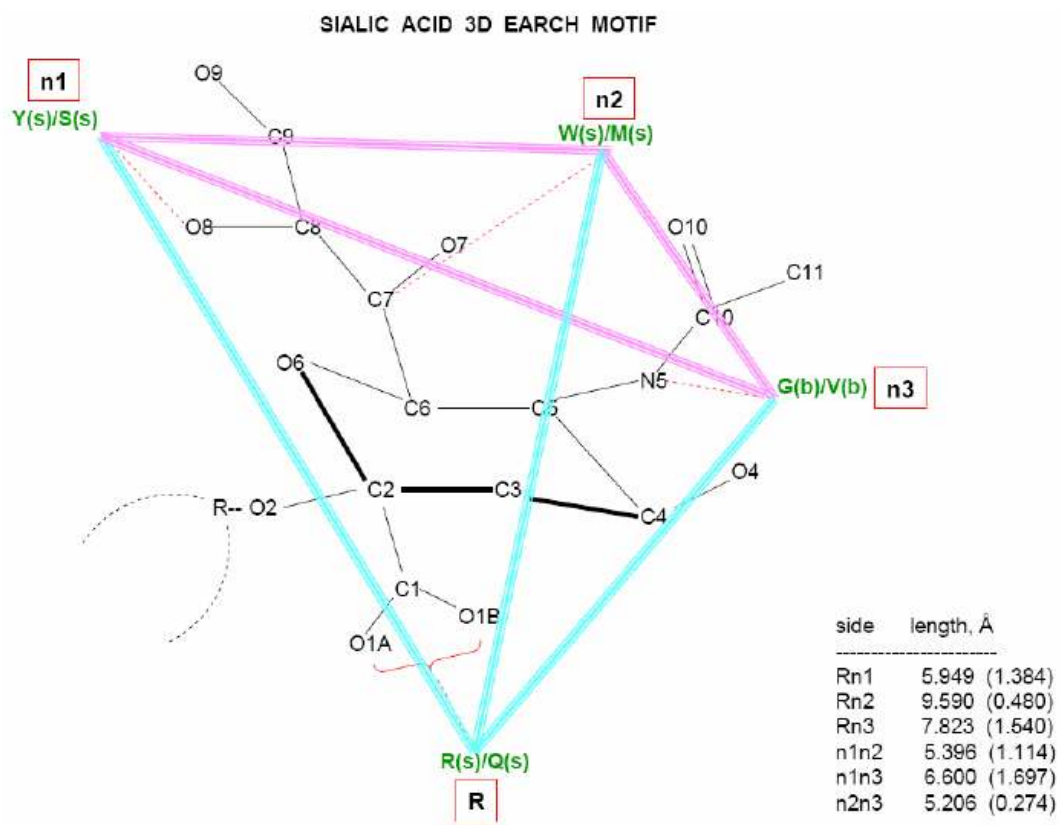


Figure 1A.

RETINOIC ACID 3D SEARCH MOTIF

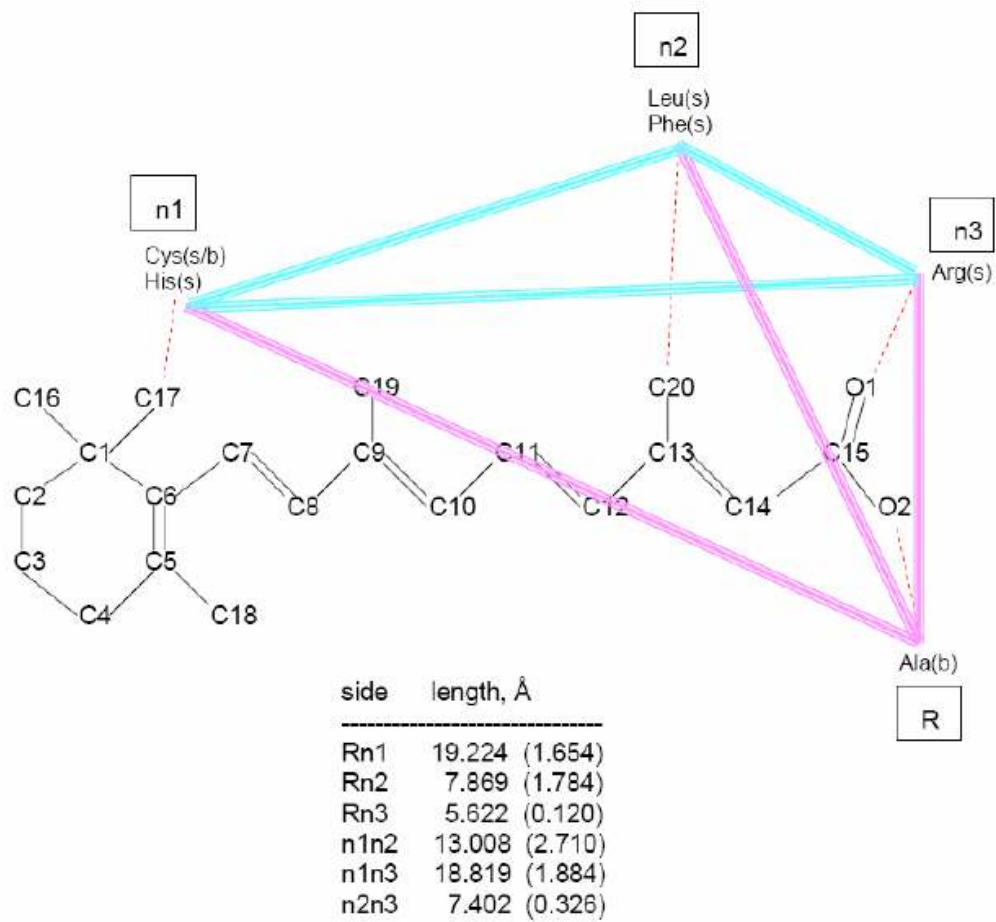


Figure 1B.

3D Search Motif #1: Heme-bound Nitric Oxide:

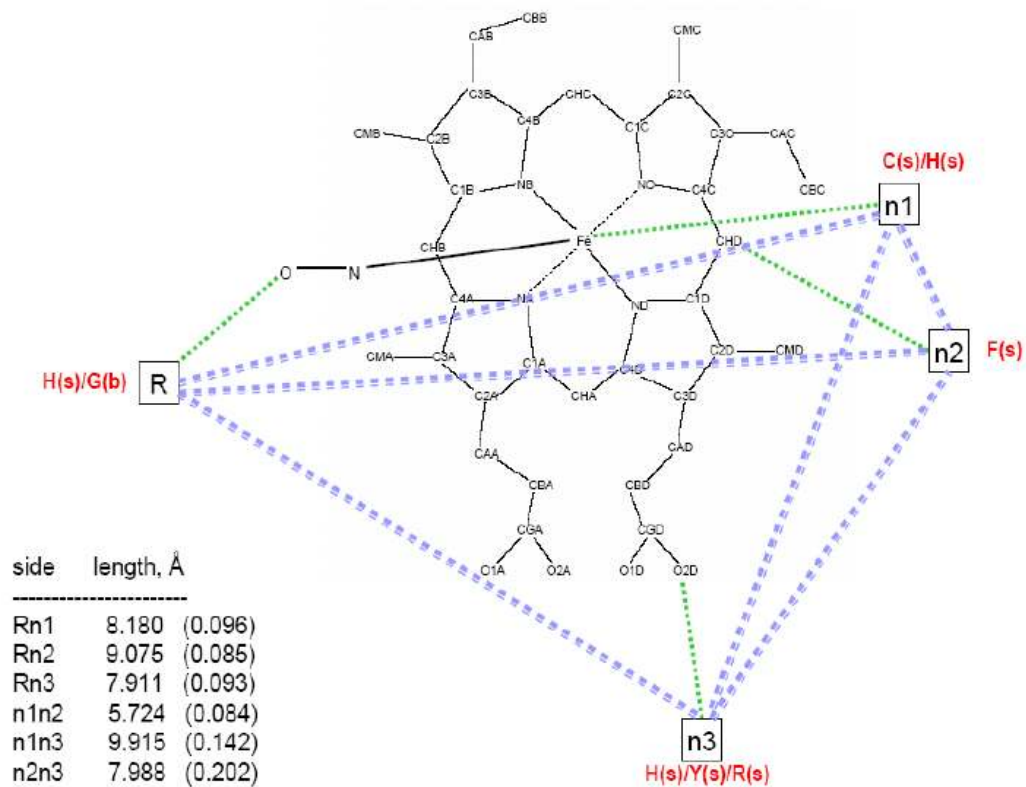


Figure 1C.

3D Search Motif #2: Non-heme Nitric Oxide:

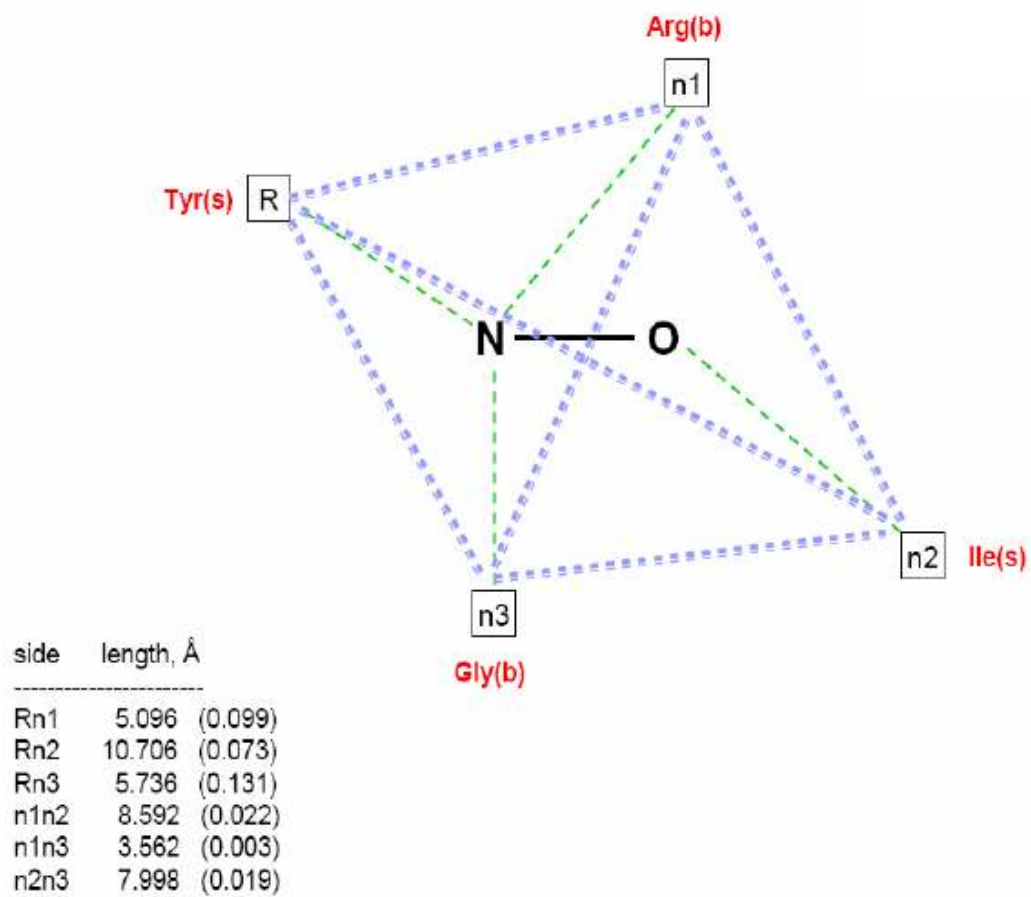


Figure 1D.

The Elimination Process Employed

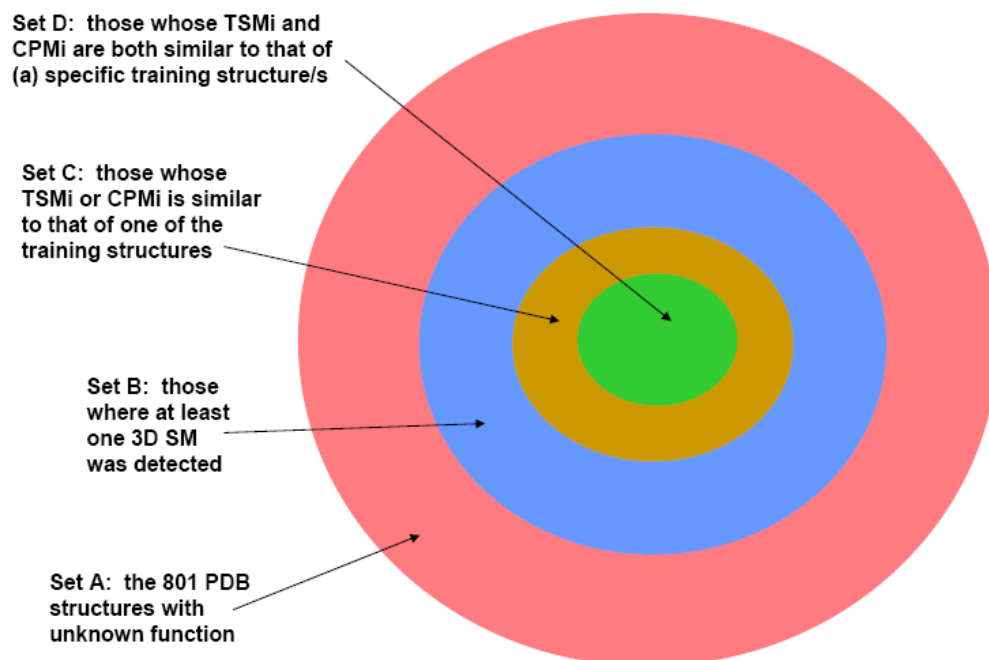


Figure 2.

TABLES:

The Training Sets

Sialic Acid Binding Site:

1JSN:A	<i>Influenza A virus</i>	Hemagglutinin HA1 chain (residues 1-325, chain A) and HA2 chain (residues 1-176, chain B) with bound N-acetyl-D-glucosamine (NAG), D-galactose (GAL), and O-sialic acid (SIA)
1JSO:A	<i>Influenza A virus</i>	Hemagglutinin HA1 chain (residues 1-325; chain A) and HA2 chain (residues 1-176; chain B) with bound N-acetyl-D-glucosamine (NAG) and O-sialic acid (SIA)
1W0O:A	<i>Vibrio cholerae</i>	Sialidase (E.C. 3.2.1.18; syn.: neuraminidase, nanase) with bound calcium ion, 2-deoxy-2,3-dehydro-N-acetyl-neuraminic acid (DAN) and O-sialic acid (SIA)
1W0P:A	<i>Vibrio cholerae</i>	Sialidase (E.C. 3.2.1.18; syn.: neuraminidase, nanase) with bound calcium ion, glycerol (GOL), 2-amino-2-hydroxymethyl-propane-1,3-diol (TRS), and O-sialic acid (SIA)
1MQN:A,D	<i>Influenza A virus</i>	Hemagglutinin HA1 chain (chains A, D, G) and HA2 chain (chains B, E, H) with bound N-acetyl-D-glucosamine (NAG), alpha-D-mannose (MAN), D-galactose (GAL) and O-sialic acid (SIA) molecules

Retinoic Acid Binding Site:

1FM9:A	<i>Homo sapiens</i>	The heterodimer of the human RXR-alpha and PPAR-gamma ligand binding domains respectively bound with 9-cis retinoic acid and GI262570 and co-activator peptides
1K74:A	<i>Homo sapiens</i>	The heterodimer of the human PPAR-gamma and RXR-alpha ligand binding domains respectively bound with GW409544 and 9-cis retinoic acid and co-activator peptides
1FBY:A,B	<i>Homo sapiens</i>	The human RXR-alpha ligand binding domain bound to 9-cis retinoic acid
1FM6:A,U	<i>Homo sapiens</i>	The heterodimer of the human RXR-alpha and PPAR-gamma ligand binding domains respectively bound with 9-cis retinoic acid and rosiglitazone and co-activator peptides
1XDK:A,E	<i>Mus musculus</i>	The RAR-beta/RXR-alpha ligand binding domain heterodimer in complex with 9-cis retinoic acid and a fragment of the TRAP220 co-activator
1XLS:A,B,C,D	<i>Homo sapiens / Mus musculus</i>	Heterodimer of the human RXR-alpha ligand binding domain and the mouse orphan nuclear receptor NR113 (syn.: constitutive androstane receptor, CAR) bound to TCPOBOP and 9-cis retinoic acid and a TIF2 peptide containing the 3rd LXXLL motifs
2ACL:A,C,E,G	<i>Homo sapiens</i>	Heterodimer of the human retinoic acid RXR-alpha and the mouse oxysterol receptor LXR-alpha (syn.: nuclear orphan receptor LXR-alpha) with bound 1-benzyl-3-(4-methoxyphenylamino)-4-phenylpyrrole-2,5-dione (L05) and retinoic acid

Heme-Bound Nitric Oxide:

1OZW:A,B	<i>Homo sapiens</i>	The ferri-, ferrous and ferrous-nitrogen oxide (heme-complexed) forms of the human heme oxygenase-1 (E.C.1.14.99.3)
1XK3:A,B	<i>Homo sapiens</i>	Heme oxygenase-1 (HO-1) Arg183Glu mutant with bound heme-complexed nitrogen oxide (NO)
1OZL:A,B	<i>Homo sapiens</i>	The ferri-, ferrous and ferrous-nitrogen oxide (heme-complexed) forms of the Asp140Ala mutant of human heme oxygenase-1 (E.C.1.14.99.3)

Unbound Nitric Oxide:

1ZGN:A,B	<i>Homo sapiens</i>	Glutathione-S-transferase pi (syn.: GST Class Pi) with bound dinitrosyl-diglutathionyl iron complex
----------	---------------------	---

Table 1.

1DI6	1J9L	1LJ7	1NNQ	1O6A	1QVV	1RZ2	1SYR	1TU9	1V70
1DI7	1JAL	1LJO	1NNW	1O6D	1QVW	1RZ3	1T06	1TUA	1V8D
1DM5	1JN1	1LPL	1NNX	1O89	1QVZ	1S12	1T07	1TUH	1V8H
1EW4	1J00	1LQL	1NO5	1O8C	1QW2	1S2X	1T0B	1TUV	1V8O
1F89	1JOG	1LXJ	1NOG	1ON0	1QY9	1S4C	1T0T	1TUV	1V8P
1FL9	1JOP	1LXN	1NPD	1OQ1	1QYA	1S4K	1T1J	1TWU	1V96
1FUX	1JOV	1M1S	1NPY	1ORU	1QYI	1S5A	1T2B	1TWY	1V99
1G2R	1JRI	1M33	1NQM	1OSC	1QZ4	1S7H	1T3U	1TXJ	1V9B
1H2H	1JRK	1M3S	1NQN	1OY1	1QZ8	1S7I	1T57	1TXL	1VAJ
1HQQ	1JSX	1M65	1NR9	1OYZ	1R0U	1S7O	1T5J	1TXZ	1VBK
1HRU	1JX7	1M68	1NRI	1OZ9	1R3D	1S8N	1T5R	1TY8	1VBV
1HTW	1JYH	1M98	1NRK	1P1L	1R4V	1S9U	1T5Y	1TZ0	1VCT
1HXL	1JZT	1MK4	1NS5	1P1M	1R5X	1SAW	1T62	1TZA	1VDH
1HXZ	1K26	1ML8	1NU0	1P5F	1R6Y	1SBK	1T6A	1TZZ	1VDW
1HY2	1K2E	1MOG	1NX4	1P8C	1R75	1SC0	1T6S	1U05	1VE3
1I36	1K3R	1MW5	1NX8	1P99	1R7L	1SD5	1T6T	1U0K	1VGG
1I60	1K4N	1MW7	1NXH	1P9I	1RC6	1SDI	1T8H	1U5W	1VGY
1I6N	1K77	1MWQ	1NXJ	1P9Q	1RCU	1SDJ	1T95	1U61	1VH0
1I9H	1K7J	1MWW	1NXZ	1PB0	1RFE	1SED	1T9F	1U69	1VH5
1IHN	1K7K	1MZG	1NY1	1PBJ	1RFZ	1SEF	1TC5	1U6L	1VH6
1IJ8	1K8F	1N1Q	1NYE	1PC6	1RI6	1SF9	1TD6	1U7I	1VH9
1ILV	1KJN	1N81	1NZA	1PD3	1RKI	1SFN	1TE5	1U7N	1VHC
1IN0	1KK9	1NC5	1NZJ	1PF5	1RKQ	1SFS	1TEL	1U84	1VHE
1IUJ	1KON	1NC7	1NZN	1PG6	1RLH	1SPX	1TLJ	1U9C	1VHF
1IUK	1KQ3	1NE2	1O0I	1PM3	1RLJ	1SG9	1TLQ	1U9D	1VHK
1IUL	1KQ4	1NE8	1O13	1PQY	1RLK	1SH8	1T00	1U9P	1VHM
1IXL	1KR4	1NF2	1O1Y	1PT5	1RTT	1SHE	1T03	1UAN	1VHN
1IZM	1KUU	1NG6	1O22	1PT7	1RTW	1SJ5	1TOV	1UC2	1VHO
1J27	1KYH	1NI9	1O3U	1PT8	1RTY	1SMB	1TP6	1UCR	1VHQ
1J2R	1KYT	1NIG	1O4T	1PUG	1RU8	1SPV	1TPX	1UE8	1VHS
1J2V	1L0B	1NIJ	1O4W	1PV5	1RV9	1SQ4	1TQ5	1UF3	1VHU
1J31	1L1S	1NJH	1O50	1PVM	1RVK	1SQE	1TQ8	1UF9	1VHY
1J3M	1L5X	1NJK	1O51	1PW5	1RW0	1SQH	1TQB	1UFA	1VI1
1J3W	1L6R	1NJR	1O5J	1Q2Y	1RW1	1SQS	1TQC	1UFB	1VI3
1J5U	1LCV	1NKQ	1O5U	1Q4R	1RW7	1SQU	1TQX	1UFH	1VI4
1J74	1LCW	1NKV	1O61	1Q77	1RXD	1SQW	1TSJ	1UJ8	1VI7
1J7D	1LCZ	1NMN	1O62	1Q7H	1RXH	1SR0	1TT4	1UMJ	1VI8
1J8B	1LDO	1NMO	1O65	1Q8B	1RXJ	1SS4	1TT7	1V30	1VIM
1J9J	1LDQ	1NMP	1O67	1Q8C	1RXK	1SU0	1TTZ	1V6H	1VIV
1J9K	1LEL	1NNH	1O69	1Q9U	1RYL	1SU1	1TU1	1V6T	1VIZ

Table 2 (part 1 of 2).

1VJ1	1VQW	1WV8	1XKF	1Y7I	1YOA	1ZC6	2A1V	2ARZ	2CUW
1VJ2	1VQY	1WV9	1XKL	1Y7M	1YOC	1ZCE	2A2L	2ASF	2CV9
1VJF	1VQZ	1WVI	1XKQ	1Y7P	1YOX	1ZD0	2A2M	2ATR	2CVB
1VJG	1VR4	1WWI	1XM5	1Y7R	1YOY	1ZE0	2A2O	2ATZ	2CVE
1VJK	1VR9	1WWP	1XM7	1Y80	1YOZ	1ZEE	2A33	2AU5	2CVL
1VJL	1VRM	1WWZ	1XMT	1Y81	1YQE	1ZHV	2A35	2AUA	2CW4
1VJU	1W8I	1WY6	1XMX	1Y82	1YQF	1ZKD	2A3N	2AUW	2CW5
1VJX	1W9A	1X6I	1XN4	1Y88	1YQH	1ZKE	2A3Q	2AV4	2CWQ
1VK0	1WD5	1X6J	1XPJ	1Y89	1YRE	1ZKI	2A5Z	2AVN	2CWY
1VK1	1WD6	1X72	1XQ4	1Y8A	1YS9	1ZKP	2A67	2AX3	2CX0
1VK5	1WDI	1X77	1XQ6	1Y8T	1YTL	1ZL0	2A6B	2AXO	2CX1
1VK8	1WDJ	1X7F	1XQ9	1Y9B	1YUD	1ZMB	2A6C	2AXP	2D2Y
1VK9	1WDT	1X7V	1XQA	1Y9E	1YV9	1ZN6	2A8E	2AZ4	2D4R
1VKA	1WDV	1X9G	1XQB	1Y9I	1YW1	1ZNP	2A9F	2AZP	2ES9
1VKB	1WEH	1XA0	1XRG	1YAC	1YW3	1ZOX	2A9S	2B0A	2ESH
1VKD	1WEK	1XAF	1XRI	1YAV	1YWF	1ZP6	2AAM	2B0C	2ESN
1VKH	1WHZ	1XB4	1XSV	1YB2	1YX1	1ZPV	2AB0	2B0R	2ETD
1VKI	1WJ9	1XBF	1XTL	1YB3	1YYV	1ZPW	2AB1	2B0V	2ETH
1VKM	1WK2	1XBV	1XTM	1YBM	1YZV	1ZPY	2ACA	2B1Y	2ETS
1VKW	1WK4	1XBW	1XTO	1YBX	1YZY	1ZQ7	2AEG	2B2P	2EUC
1VL0	1WKC	1XBX	1XUV	1YCD	1YZZ	1ZS7	2AEU	2B2Z	2EUI
1VL4	1WLU	1XBY	1XV2	1YCY	1Z0P	1ZS0	2AEV	2B30	2EVE
1VL5	1WLV	1XBZ	1XVS	1YDF	1Z1S	1ZSW	2AFC	2B33	2EVR
1VL7	1WLZ	1XCC	1XW8	1YDH	1Z40	1ZTC	2AH5	2B3M	2EVV
1VLY	1WM6	1XDI	1XWM	1YDM	1Z67	1ZTD	2AH6	2B3N	2EWO
1VM0	1WMM	1XE1	1XX7	1YDW	1Z6M	1ZTP	2AI4	2B41	2EWC
1VMF	1WN3	1XE7	1XXL	1YE5	1Z6N	1ZTV	2AJ2	2B4A	2EWR
1VMH	1WN9	1XE8	1XY7	1YEM	1Z7A	1ZUP	2AJ6	2B4W	2F06
1VMJ	1WNA	1XFI	1Y0H	1YEY	1Z7U	1ZVP	2AJ7	2B6C	2F20
1VP2	1WOL	1XFJ	1Y0K	1YF9	1Z84	1ZWJ	2ALI	2B6E	2F22
1VP4	1WOZ	1XFS	1Y0N	1YHF	1Z85	1ZWY	2AMH	2B8M	2F4L
1VP8	1WPB	1XG7	1Y0Z	1YKW	1Z8H	1ZX3	2AMU	2BBE	2F4N
1VPB	1WR2	1XG8	1Y12	1YLK	1Z90	1ZX5	2AO9	2BDT	2F4Z
1VPH	1WSC	1XHN	1Y1X	1YLL	1Z94	1ZX8	2AP3	2BDV	2F9C
1VPQ	1WTY	1XHO	1Y2I	1YLM	1Z9T	1ZXJ	2AP6	2BE4	2FBL
1VPV	1WU8	1XI6	1Y5H	1YLN	1ZBM	1ZXO	2APJ	2C5Q	2FBM
1VPY	1WUE	1XI8	1Y63	1YLO	1ZBO	1ZXU	2APL	2COH	2FDS
1VPZ	1WUF	1XIZ	1Y6Z	1Y LX	1ZBP	1ZZM	2AQW	2CSL	2FE1
1VQR	1WUS	1XJC	1Y71	1YN4	1ZBR	2A13	2AR1	2CU5	2FFG
1VQS	1WV3	1XK8	1Y7H	1YN5	1ZBS	2A15	2ARH	2CU6	2FFI
									2FFM

Table 2 (part 2 of 2).

PDB ID [*]	DESCRIPTION
104M	Sperm whale (<i>Physeter catodon</i>) skeletal muscle myoglobin (heme-iron(II)-bound) with bound N-butyl isocyanide and sulfate ion at pH 7.0
1ASH	Iron(II)-protoporphyrin IX-bound hemoglobin domain I from <i>Ascaris suum</i> with bound dioxygen at 2.2 Å resolution
1B3B	Structure of glutamate dehydrogenase from <i>Thermotoga maritima</i> with mutations N97D and G378K
1BRF	Structure of Rubredoxin with bound Fe(III) from <i>Pyrococcus furiosus</i> at 0.95 Å resolution
1CBN	Structure of the hydrophobic protein crambin from the seed of <i>Crambe abyssinica</i> (Abyssinian cabbage) at 130°K and at 0.63 Å resolution
1CKO	Structure of mRNA capping enzyme from <i>Chlorella</i> virus PBCV-1 in complex with the CAP analog GpppG
1CRP	NMR structure (n=20) of human C-H-Ras p21 protein (catalytic domain, res. 1-166) complexed with GDP and MG
1EWK	Structure of the metabotropic glutamate receptor subtype 1 from <i>Rattus norvegicus</i> complexed with glutamate
1F3O	Structure of MJ0796 ATP-binding cassette with bound Mg-ADP from <i>Methanococcus jannaschii</i>
1FW5	Solution structure of membrane binding peptide of Semliki forest virus mRNA capping enzyme NSP1
1HWY	Glutamate dehydrogenase from <i>Bos taurus</i> complexed with NAD and 2-oxoglutarate
1JFF	Refined structure of bovine (<i>Bos taurus</i>) α - β tubulin from zinc-induced sheets stabilized with taxol
1MJJ	Structure of the complex of the Fab fragment of esterolytic antibody MS8-12 and the transition-state analog, N-[[2-[[[1-(4-carboxybutanoyl)amino]-2-phenylethyl]-hydroxyphosphinyl]oxy]acetyl]-2-phenylethylamine
1MV5	Structure of the ATP-binding domain of the multidrug resistance ABC transporter and permease protein from <i>Lactococcus lactis</i> with bound ADP, ATP and Mg ion
1NQT	Structure of glutamate dehydrogenase from <i>Bos taurus</i> with bound ADP
1PE6	Structure of papain (E.C.4.3.22.2) from the papaya fruit (<i>Carica papaya</i>) latex complexed with E-64-C ((2S,3S)-3-(1-(N-(3-methylbutyl)amino)heptylcarboxyl)oxirane-2-carboxylate) at 2.1 Å resolution
1RQ7	<i>Mycobacterium tuberculosis</i> FTSZ (filamenting temperature-sensitive mutant Z) in complex with GDP
1SVS	Structure of the K180P mutant of G1 α subunit bound to GPPNHP (phosphoaminophosphonic acid-guanylate ester)
1TUB	Electron diffraction structure of <i>Sus scrofa</i> (pig) tubulin α - β dimer with bound GTP, GDP and taxotere
1TWY	Structure of a hypothetical ABC-type phosphate transporter from <i>Vibrio cholerae</i> O1 Biovar eltor
1Z3C	mRNA cap (guanine-N7) methyltransferase from the encephalitozoon <i>Cuniculi</i> complexed with AzoAdoMet

^{*}These negative control structures were used for sialic acid, retinoic acid, and heme-bound and unbound nitric oxide; negative control structures used for ATP (ser/thr protein kinases) and GTP (small, Ras-type G-proteins) are enumerated and discussed in Reyes, V.M., 2008a.

Table 3.

Species Distribution of the 801 Application Structures

Source organism	No. structures	% of Total	Source organism	No. structures	% of Total
<i>Escherichia coli</i>	88	10.99	<i>Xanthomonas campestris</i>	02	0.25
<i>Thermotoga maritima</i>	63	7.86	<i>Vibrio parahaemolyticus</i>	02	0.25
<i>Thermus thermophilus</i>	56	6.99	<i>Sulfolobus solfataricus</i>	02	0.25
<i>Bacillus subtilis</i>	48	5.99	<i>Streptococcus mutans</i>	02	0.25
<i>Pseudomonas aeruginosa</i>	38	4.74	<i>Salmonella enterica</i>	02	0.25
<i>Haemophilus influenzae</i>	26	3.24	<i>Rattus norvegicus</i>	02	0.25
<i>Archaeoglobus fulgidus</i>	23	2.87	<i>Pseudomonas putida</i>	02	0.25
<i>Pyrococcus furiosus</i>	20	2.50	<i>Plasmodium yoelii</i>	02	0.25
<i>Pyrococcus horikoshii</i>	20	2.50	<i>Neisseria meningitidis</i>	02	0.25
<i>Arabidopsis thaliana</i>	20	2.50	<i>Methanosarcina mazei</i>	02	0.25
<i>Staphylococcus aureus</i>	18	2.25	<i>Erwinia carotovora</i>	02	0.25
<i>Homo sapiens</i>	18	2.25	<i>Deinococcus radiodurans</i>	02	0.25
<i>Saccharomyces cerevisiae</i>	17	2.12	<i>Chromobacterium violaceum</i>	02	0.25
<i>Mycobacterium tuberculosis</i>	16	1.99	<i>Caulobacter crescentus</i>	02	0.25
<i>Vibrio cholerae</i>	13	1.62	<i>Capra hircus</i>	02	0.25
<i>Enterococcus faecalis</i>	13	1.62	<i>Bordetella bronchiseptica</i>	02	0.25
<i>Bacillus cereus</i>	13	1.62	<i>Bacillus anthracis</i>	02	0.25
<i>Agrobacterium tumefaciens</i>	13	1.62	Uncultured bacterium	01	0.12
<i>Streptomyces avidinii</i>	12	1.50	<i>Trypanosoma brucei</i>	01	0.12
<i>Thermoplasma acidophilum</i>	11	1.37	<i>Trypanosoma cruzi</i>	01	0.12
<i>Leishmania major</i>	10	1.25	<i>Toxoplasma gondii</i>	01	0.12
<i>Bacillus stearothermophilus</i>	10	1.25	Synthetic protein	01	0.12
<i>Streptococcus pyogenes</i>	08	1.00	<i>Streptomyces glaucescens</i>	01	0.12
<i>Streptococcus pneumoniae</i>	08	1.00	<i>Schizosaccharomyces pombe</i>	01	0.12
<i>Salmonella typhimurium</i>	08	1.00	<i>Sars coronavirus</i>	01	0.12
<i>Pyrobaculum aerophilum</i>	08	1.00	<i>Rhodospseudomonas palustris</i>	01	0.12
<i>Plasmodium falciparum</i>	07	0.87	<i>Pseudomonas syringae</i>	01	0.12
<i>Nitrosomonas europaea</i>	07	0.87	<i>Plasmodium berghei</i>	01	0.12
<i>Methanobacterium thermoautotrophicum</i>	07	0.87	<i>Plasmodium vivax</i>	01	0.12
<i>Bacteroides thetaiotaomicron</i>	07	0.87	<i>Plasmodium yoelii</i>	01	0.12
<i>Bacillus halodurans</i>	07	0.87	<i>Plasmodium knowlesi</i>	01	0.12
<i>Shewanella oneidensis</i>	06	0.75	<i>Mycoplasma genitalium</i>	01	0.12
<i>Methanococcus jannaschii</i>	06	0.75	<i>Moorella thermoacetica</i>	01	0.12
<i>Helicobacter pylori</i>	06	0.75	<i>Listeria monocytogenes</i>	01	0.12
<i>Aquifex aeolicus</i>	06	0.75	<i>Listeria innocua</i>	01	0.12
<i>Sulfolobus tokodaii</i>	05	0.62	<i>Leishmania donovani</i>	01	0.12
<i>Shigella flexneri</i>	05	0.62	<i>Klebsiella pneumoniae</i>	01	0.12
<i>Ovis aries</i>	05	0.62	<i>Influenza A</i>	01	0.12
<i>Mus musculus</i>	05	0.62	<i>Hydra vulgaris</i>	01	0.12
<i>Methanothermobacter</i>	05	0.62	<i>Halobacterium salinarum</i>	01	0.12
<i>Gallus gallus</i>	05	0.62	<i>Drosophila melanogaster</i>	01	0.12
<i>Caenorhabditis elegans</i>	05	0.62	<i>Desulfovibrio vulgaris</i>	01	0.12
<i>Aeropyrum pernix</i>	05	0.62	<i>Danio rerio</i>	01	0.12
<i>Nostoc punctiforme</i>	04	0.50	<i>Cryptosporidium parvum</i>	01	0.12
<i>Clostridium acetobutylicum</i>	04	0.50	<i>Citrobacter braakii</i>	01	0.12
<i>Campylobacter jejuni</i>	04	0.50	<i>Camelus dromedarius</i>	01	0.12
<i>Bacillus stearothermophilus</i>	04	0.50	<i>Bradyrhizobium japonicum</i>	01	0.12
<i>Porphyromonas gingivalis</i>	03	0.37	<i>Bordetella parapertussis</i>	01	0.12
<i>Nicotiana tabacum</i>	03	0.37	<i>Bordetella pertussis</i>	01	0.12
<i>Mycoplasma pneumoniae</i>	03	0.37	<i>Bacteriophage lambda</i>	01	0.12
<i>Escherichia coli & Shigella</i>	03	0.37	<i>Bacillus brevis</i>	01	0.12
<i>Clostridium thermocellum</i>	03	0.37	<i>Arthrospira maxima</i>	01	0.12
<i>Chlorobium tepidum</i>	03	0.37	<i>Acinetobacter sp.</i>	01	0.12

Table 4.

GTP-binding small Ras-type G-proteins

CPM		TSM			
1o3y:A	8.0330	1m7b:A	16.6906		
1nvu:Q	10.2041	1e96:A	17.7361		
1n6l:A	10.3577	1loo:A	23.0242		
2rap:~	10.6095	1n6l:A	27.6453		
1m7b:A	16.4748	1nvu:Q	30.6122		
1e96:A	16.5826	2rap:~	31.3017		
1loo:A	16.7015	1o3y:A	31.6817		
1vhq:B	2.6710	2b30:C	2.4272		
* 1vhq:A	3.0928	2b30:D	2.4713		
* 1oy1:D	3.2967	2b30:B	2.5652		
* 1vim:C	3.3058	2b30:A	2.6979		
* 1oy1:C	3.4216	* 1xtl:B	18.3979		
* 1oy1:B	4.3478	* 1ru8:A	19.4886		
* 1sg9:B	5.6351	* 1ru8:B	19.4886		
* 1oy1:A	5.6747	1vim:C	42.4931		
* 1to0:B	6.0124	1sg9:B	45.7737		
* 1to0:G	6.3660	1oy1:A	51.0719		
* 1ru8:A	7.5000	1oy1:B	53.7084		
* 1ru8:B	7.5000	1oy1:D	56.2379		
* 1to0:D	8.5863	1oy1:C	56.6172		
* 1xtl:B	17.7817	1vhq:A	56.8299		
2b30:A	25.6966	1vhq:B	58.3713		
2b30:B	25.9620	1to0:D	66.5221		
2b30:C	26.3019	1to0:G	75.5084		
2b30:D	26.3019	1to0:B	76.7462		
1oy1	A-219	K-132	G-131	D-90	AAAA
1oy1	A-219	K-132	G-131	D-90	BBBB
1oy1	A-219	K-132	G-131	D-90	CCCC
1oy1	A-219	K-132	G-131	D-90	DDDD
* 1ru8	A-59	K-68	G-69	D-56	AAAA
* 1ru8	A-59	K-68	G-69	D-56	BBBB
1sg9	G-248	K-202	G-225	D-250	BBBB
1to0	G-60	K-56	G-112	D-57	BBBB
1to0	G-60	K-56	G-112	D-57	DDDD
1to0	G-60	K-56	G-112	D-57	GGGG
1vhq	A-219	K-132	G-131	D-90	AAAA
1vim	A-118	K-112	G-87	D-114	CCCC
* 1xtl	A-169	K-53	G-52	D-171	BBBB

Table 5 (part 1 of 7)

ATP-binding ser/thr Protein Kinases									
CPM					TSM				
1fin:A	-0.0000	2phk:A	16.9862	1gol:	17.9938	1gol:	17.5801	1jst:C	23.0029
1fin:C	-0.0000	1phk:	17.5864	1ql6:A	18.3263	1ql6:A	17.8855	1jst:A	23.6812
1qmx:A	-0.0000	1hck:	17.5949	1jst:C	19.3643	2phk:A	19.3045	1fin:A	-100.0000
1qmx:C	-0.0000	1h39:A	17.6445	1jst:A	19.6570	1phk:	19.5603	1fin:C	-100.0000
			17.8587			1hck:	21.3080	1qmx:A	-100.0000
						1h39:A	22.3555	1qmx:C	-100.0000
						1h38:A	22.6552		
1wzf:A	2.2743	1ro8:B	9.1477	1v99:D	11.9954	1t3c:B	15.9080	1gpe:A	10.8896
1wzf:B	2.2743	1ygf:A	9.1664	1jcl:F	12.1921	1t3c:A	16.3468	1w8:D	12.3952
1yph:B	2.3828	1pvr:B	9.1713	1e99:A	12.3414	14gl:B	16.3899	1w8:A	12.6362
1e81:C2	3.8404	1lao:	9.1807	1e8a:A	12.3414	14gl:C	16.7031	1w8:C	12.6362
1yph:A	4.3059	1ocx:B2	9.3759	1v9b:D	12.3814	1off:B	16.7429	1w8:B	12.6362
1e81:C1	4.4243	1pvr:A	9.3833	1e99:F	12.4138	14gl:A	16.8323	1e81:D	12.6362
1e81:B2	4.8727	1v97:A1	9.4038	1e81:A	12.4813	143c:C	16.8994	1w8:E	12.6362
1ocx:B1	5.8987	1tt7:A2	9.4566	1e80:A	12.5079	1t3c:D	16.9052	1gpe:B	14.3365
1v97:A2	5.2016	1ocx:A2	9.7079	1ocx:B3	12.6645	1t9f:D	17.0366	1w8:F3	14.4737
1w8e:A2	9.4608	1e8a:B	9.8382	1e8a:D	12.6874	14gl:F	17.0366	1e81:A	16.2448
1e81:B1	9.6727	1ag7:C3	9.9871	1e81:D	12.7650	1w8e:C	17.0469	1e81:C	16.4669
1v15:B	9.6920	1k3a:A	10.0966	1v99:D	12.8131	1w8e:B	17.1162	1e81:D	16.2800
1w8j:D	9.8992	1w8p:B2	10.1288	1e8a:F	12.8131	1w8e:A	17.1428	1e81:F3	16.2800
1e13:D	9.8148	1h3e:	10.1844	1v9b:D	12.8468	1w8e:A	17.2448	1e81:A	16.4669
1e5q:A2	9.8180	1tt7:D	10.3677	1e81:D	12.8794	1off:C	17.5266	1e81:A	16.4669
1e8j:A2	9.8180	1w8p:A2	10.4149	1e8j:A	13.8438	1off:A	17.7488	1e81:F2	16.7985
1e8j:D	9.8180	1e8a:B	10.4408	1e99:B	13.1034	1w8e:B	17.7677	1e81:F	16.8122
1v97:D	9.1224	1ag7:A	10.4650	1v9b:D	13.1898	1w8e:D	17.7988	1e81:F	17.0366
1e5q:D	9.1987	1e8a:A	10.5455	1e80:D	13.2660	1w8e:D	17.8055	1e81:D	17.0366
1v97:A	6.1237	1v9a:D	10.3928	1w8p:B1	13.3398	1gpe:B	18.1287	1e81:C	17.2448
1e5q:B	6.2288	1w8p:C2	10.5572	1w8p:C1	13.4997	1yph:F	18.9089	1e81:F	17.3333
1v97:A	6.3336	1ag7:D	10.6922	1w8e:A3	13.6519	1yph:C	19.2974	1e81:B	17.3208
1e5q:B	6.4390	1w8p:F2	10.7928	1w8p:A2	13.7038	1gpe:B	19.4167	1e81:B	17.3208
1w8p:B1	7.2088	1ag7:C	10.7940	1e8a:C	13.7230	1e8a:A	19.8847	1e81:B	17.6887
1y8c:A	7.2923	1v97:H	10.8434	1w8e:F3	13.7550	1tt7:B3	22.7953	1e81:C	16.3333
1w8j:B2	7.3881	1v9a:B	10.8621	1e80:C	13.8384	1v97:B4	22.7953	1e81:D	19.6370
1y81:A	7.8033	1w8e:B	11.2749	1e80:C	13.8408	1y8e:A1	22.8828	1e81:E	20.2747
1e8k:D	7.8641	1v97:I	11.2875	1gpe:D	13.8626	1y8e:A2	22.8619	1e81:F	20.2747
1y8j:A	7.8687	1v97:A1	11.3134	1y8j:A	14.1724	1tt7:C2	22.8907	1e81:A	21.1284
1y8j:B	7.8687	1v97:A3	11.3134	1y8j:B	14.2728	1tt7:C2	22.8785	1e81:A	21.1284
1y8k:A	8.8629	1e8a:A	11.3427	1e57:D	14.5195	1y8e:C	23.2382	1e81:A	22.1884
1y8k:D	8.8629	1e8a:B	11.3846	1e19:A	14.6614	1tt7:B2	23.2529	1e81:B	22.4596
1y81:B	8.8829	1w87:C2	11.4048	1e81:B	14.6887	1y8e:B1	23.3152	1e81:A	22.6887
1w8e:A	8.8602	1e8a:A	11.4287	1e81:D	14.6687	1y8e:B2	23.3152	1e81:C1	22.7837
1w8p:A	8.5925	1ag7:B	11.4264	1e81:F	14.6687	1tt7:C1	23.4153	1w8e:D	22.8216
1w87:C2	8.6340	1e8j:A	11.4373	1y8j:A	14.7028	1e8a:A	24.0088	1tt7:D1	22.5021
1w87:B1	8.7429	1e81:A	11.4828	1e8j:B	14.8823	1e8a:A	24.1278	1w87:B2	22.8021
1w87:C1	8.8273	1w87:B2	11.5335	1e8j:A	15.8335	1e81:B	25.2788		
1w87:A2	8.8428	1y8e:C	11.6771	1y8j:B	16.2088	1e8j:B	27.8773		
1e8k:C	8.8638	1w87:C2	11.7288	1y8j:D	16.2827	1e8j:A	28.0728		
1y87:F	9.8285	1w87:A2	11.8759	1w8e:F2	15.3809	1e8j:D	28.6249		
1v97:A	9.1477	1v97:A	11.9185	1y8j:A	15.5806	1e8j:C	29.1335		

[NOTE: only structures of CPM and TSM values within 13.8 units of those of training structures are shown]

1f19	V-71	E-94	L-86	E-113	AAAA	1vk0	V-109	E-157	L-43	E-39	AAAA
1l1xn	V-34	E-55	L-50	E-48	BBBB	1vk0	V-109	E-157	L-43	E-39	CCCC
1mww	V-97	D-58	L-90	E-85	AAAA	1vk0	V-109	E-157	L-43	E-39	DDDD
1mww	V-97	D-58	L-90	E-85	BBBB	1vph	V-100	E-133	L-135	E-133	CCCC
1mww	V-97	D-58	L-90	E-85	CCCC	1vph	V-100	E-133	L-135	E-133	FFFF
1nf2	V-51	E-19	L-13	D-10	AAAA	1wm6	V-13	E-81	M-1	D-3	AAAA
1nf2	V-351	E-319	L-313	D-310	BBBB	1wm6	V-13	D-3	L-16	E-20	FFFF (1)
1nf2	V-651	E-619	L-613	D-610	CCCC	1wm6	V-13	D-3	L-53	E-20	FFFF (2)
1o1y	V-134	E-175	L-213	E-209	AAAA	1wm6	V-23	D-3	L-16	E-20	FFFF (3)
1pm3	V-26	E-5	M-1	D-29	BBBB	1xbv	V-47	D-62	L-38	E-42	AAAA
1r5x	V-33	E-13	L-7	E-36	AAAA	1xbv	V-47	D-62	L-38	E-42	BBBB
1r5x	V-33	E-13	L-7	E-36	BBBB	1xbx	V-47	D-62	L-38	E-42	AAAA
1rki	V-44	D-29	L-48	E-52	AAAA	1xbx	V-47	D-62	L-38	E-42	BBBB
1rkq	V-238	D-259	L-16	D-12	AAAA	1xbx	V-47	D-62	L-38	E-42	AAAA
1rkq	V-238	D-259	L-16	D-12	BBBB	1xbx	V-47	D-62	L-38	E-42	BBBB
1sbk	V-59	E-84	L-131	E-84	DDDD	1xbx	V-47	D-62	L-38	E-42	AAAA
1t57	V-172	E-117	L-95	E-131	CCCC	1xbz	V-47	D-62	L-38	E-42	AAAA
1tq8	V-124	D-152	L-154	D-152	AAAA	1xrg	V-78	E-119	L-117	D-82	AAAA (1)
1tq8	V-124	D-152	L-154	D-152	BBBB	1y9e	V-38	D-68	L-65	D-99	AAAA (1)
1tq8	V-124	D-152	L-154	D-152	CCCC	1y9e	V-38	D-68	L-65	D-99	AAAA (2)
1tq8	V-124	D-152	L-154	D-152	DDDD	1y9e	V-38	D-68	L-65	D-99	BBBB (1)
1tq8	V-124	D-152	L-154	D-152	FFFF	1y9e	V-38	D-68	L-65	D-99	BBBB (2)
1tt7	V-38	D-68	L-65	D-99	BBBB (1)	1y9e	V-38	D-68	L-65	D-99	DDDD
1tt7	V-38	D-68	L-65	D-99	BBBB (2)	1yyv	V-99	E-97	L-76	D-73	AAAA
1tt7	V-96	D-68	L-65	D-99	BBBB (3)	1yyv	V-99	E-97	L-76	D-73	BBBB
1tt7	V-96	D-68	L-65	D-99	BBBB (4)	2c5q	V-229	D-225	L-208	E-204	AAAA (1)
1tt7	V-38	D-68	L-65	D-99	CCCC (1)	2c5q	V-229	D-225	L-208	E-204	AAAA (2)
1tt7	V-96	D-68	L-65	D-99	CCCC (2)	2c5q	V-229	D-225	L-208	E-204	BBBB
1u9p	V-52	E-59	L-77	E-73	AAAA	2c5q	V-229	D-225	L-208	E-204	CCCC
1ucr	V-9	E-2	L-46	E-50	AAAA (2)	2c5q	V-229	D-225	L-208	E-204	DDDD
1ucr	V-9	E-53	L-46	E-50	AAAA (3)	2c5q	V-229	D-225	L-208	E-204	EEEE
1ucr	V-9	E-2	L-46	E-50	BBBB (2)	2cv1	V-104	E-116	L-77	E-116	BBBB
1ucr	V-9	E-53	L-46	E-50	BBBB (3)	2cv1	V-104	E-116	L-77	E-116	CCCC
						2cv1	V-104	E-116	L-77	E-116	FFFF
						2f41	V-194	E-32	L-34	D-173	AAAA
						2f41	V-194	E-32	L-34	D-173	BBBB
						2f41	V-194	E-32	L-34	D-173	DDDD

Table 5 (part 2 of 7)

sialic acid-binding proteins

CPM		TSM	
1w0o:A	2.3854	1jso:A	52.4113
1w0p:A	2.3854	1jsn:A	52.5309
1mqn:A	14.1443	1mqn:A	52.8660
1mqn:D	14.3092	1mqn:D	52.8783
1jsn:A	15.1853	1w0o:A	92.1400
1jso:A	15.3448	1w0p:A	92.2602
* 1vka:A	4.4976	* 1t62:B	16.4414
* 1iuk:A	5.1423	* 1j7d:A	16.4568
* 1sqh:A	5.5626	* 1j74:A	16.6065
* 1f89:A	7.2532	* 1vdh:E	16.7980
* 1f89:B	7.2532	* 1qyi:A	19.4749
* 1mzg:B	7.7333	* 1wue:B	20.4061
* 1ywf:A	7.8041	* 1wue:A	20.6489
* 1mzg:A	8.4137	* 1z94:F	21.6438
* 1y6z:B	8.6742	* 1tc5:D	24.7067
* 1nxj:B	9.9203	* 1tc5:C	24.9828
* 1o62:A	10.0508	* 1tc5:B	25.1026
* 2arl:A	10.7170	* 1tc5:A	25.1029
* 1te5:B	11.5752	1wr2:A	25.7388
* 1uc2:A	12.1043	1y7p:C	30.5085
* 1uc2:B	12.1841	1y7p:A	31.4373
* 1t62:A	12.6492	1pt7:B	35.9453
* 1yv9:A	13.6226	1pt7:A	36.1629
* 1wk4:C	14.9818	1pt8:A	36.6625
* 1sfs:A	15.5316	1pt5:A	36.7537
* 1vdh:D	15.5665	1pt5:B	36.7848
* 1wuf:A	16.0896	1pt8:B	36.9403
* 1wuf:B	16.1575		
		1y7p:A	1.2232
		1y7p:C	1.3810
		1pt8:B	1.7413
		1pt8:A	1.7680
		1pt5:A	1.7724
		1pt7:A	1.7724
		1pt7:B	1.7724
		1pt5:B	1.8035
		1tc5:A	2.3320
		1tc5:B	2.3940
		1tc5:C	2.5465
		1tc5:D	2.6225
		1z94:F	4.8402
		1qyi:A	7.7767
		1wr2:A	10.2633
		1wk4:C	14.4000
		1wue:A	14.4981
		1wue:B	14.5516
		1yv9:A	14.9849
		1wuf:A	17.2437
		1wuf:B	17.2777
		1nxj:B	18.3348
		1t62:B	20.5706
		1te5:B	20.7348
		1sfs:A	23.2239
		1t62:A	25.3779
		1uc2:B	27.4541
		1uc2:A	27.8532
		1f89:B	28.6851
		1f89:A	28.8255
		1j74:A	31.5884
		1mzg:A	31.8142
		1j7d:A	32.0144
		1ywf:A	32.9925
		1vdh:E	35.6158
		1o62:A	37.2927
		1vdh:D	38.1281
		1mzg:B	38.3111
		2arl:A	39.2444
		* 1vka:A	40.0957
		* 1iuk:A	53.0762
		* 1y6z:B	62.9867
		* 1sqh:A	64.3911

sialic acid-binding proteins (cont'd.)

1f89	R-226	Y-235	W-204	G-236	AAAA
1f89	R-526	Y-535	W-504	G-536	BBBB
* 1iuk	R-135	Y-35	M-127	V-128	AAAA
1j74	R-61	Y-63	M-126	G-52	AAAA
1j7d	R-61	Y-63	M-126	G-52	AAAA
1mzg	Q-49	S-47	W-56	V-55	AAAA
1mzg	Q-49	S-47	W-56	V-55	BBBB
1nxj	R-130	S-40	W-90	V-54	BBBB
1o62	Q-39	S-40	M-242	V-41	AAAA
1qyi	R-17	Y-207	W-184	V-21	AAAA
1sfs	Q-12	S-10	W-32	V-14	AAAA
* 1sqh	Q-99	S-97	W-98	G-80	AAAA
1t62	Q-1080	S-1079	M-1027	G-1077	AAAA
1t62	Q-2080	S-2079	M-2027	G-2077	BBBB
1tc5	Q-99	Y-41	M-39	V-40	AAAA
1tc5	Q-99	Y-41	M-39	V-40	BBBB
1tc5	Q-99	Y-41	M-39	V-40	CCCC
1tc5	Q-99	Y-41	M-39	V-40	DDDD
1te5	Q-239	Y-191	W-247	V-245	BBBB
1uc2	R-27	Y-29	M-63	V-62	AAAA
1uc2	R-27	Y-29	M-63	V-62	BBBB
1vdh	R-52	Y-62	W-51	V-48	DDDD
1vdh	R-52	Y-62	W-51	V-48	EEEE
* 1vka	R-84	S-55	M-48	G-81	AAAA
1wk4	R-80	S-82	W-128	V-127	CCCC
1wue	R-1235	S-1259	W-1288	V-1287	AAAA
1wue	R-2235	S-2259	W-2288	V-2287	BBBB
1wuf	Q-1088	S-1271	M-1270	G-1269	AAAA
1wuf	Q-2088	S-2271	M-2270	G-2269	BBBB
* 1y6z	R-72	Y-74	W-5	V-99	BBBB
1yv9	Q-219	S-216	M-189	G-217	AAAA
1ywf	R-235	Y-238	M-126	G-230	AAAA
1z94	Q-136	S-133	W-130	G-129	FFFF
2ar1	R-77	Y-80	M-106	V-107	AAAA

Table 5 (part 3 of 7)

retinoic acid-binding proteins

CPM				TSM			
2acl:A	~0.0000	1xls:C	22.4501	1k74:A	9.2930	1xdk:A	15.5882
2acl:C	~0.0000	1xls:A	22.5071	1fm9:A	9.3501	1xdk:E	15.6471
2acl:E	~0.0000	1xls:B	22.5071	1fm6:U	12.7708	1fby:A	16.6471
2acl:G	~0.0000	1xls:D	22.5071	1fm6:A	13.4550	1fby:B	20.9928
1fby:B	19.7966	1fm6:U	23.3751	1xls:A	15.2137	2acl:A	~100.0000
1xdk:A	22.0000	1fm6:A	23.5462	1xls:C	15.2707	2acl:C	~100.0000
1xdk:E	22.0000	1fm9:A	25.0855	1xls:D	15.2707	2acl:E	~100.0000
1fby:A	22.0985	1k74:A	25.3136	1xls:B	15.3276	2acl:G	~100.0000
1vhc:B	4.2318	1vkb:A	9.9835	1vdh:D	15.9606		
1sdi:A	4.3452	2a3q:A	10.1751	1vdh:A	16.1084		
1y7i:A	4.3655	2aca:B	10.2232	1u6l:B	16.5953		
1y7i:B	4.4843	1zn6:A	10.2689	1x1h:A	17.2563		
1sh8:A	5.1581	1z6n:A	10.4732	1yey:C	18.3673		
1u5w:H	5.2221	1k3r:A	10.9609	1qya:B	18.4687		
1yx1:A2	5.2580	1v6h:A	10.9890	1yey:B	18.5162		
1u5w:E	5.3200	1k3r:B	11.0206	1nx4:C	18.8641		
1u5w:G	6.4822	1mwq:B	11.3253	1vim:C	18.8705		
1kyh:A	6.7399	1mwq:A	11.5202	1nx8:C	18.9040		
1o65:A	7.0893	1v6h:C	11.5854	1nx4:A	19.0574		
1xfj:A	7.1391	1rw0:A	12.3317	1vnh:A	19.0813		
1tlj:B	7.1521	1zzm:A	12.4571	1z6m:A	19.2542		
1wlz:D	7.2617	1v6h:B	12.5152	1y8t:A	19.4195		
1zkd:A	7.3617	1rw0:B	12.6010	1nx4:B	19.4280		
1zkd:B	7.3921	1zoc6:A	13.3235	1tul:B	20.3151		
1yx1:A1	7.5184	1u7i:B	13.6452	1y8t:B	20.5441		
1vho:A	7.5833	1vp2:B	13.7492	1u69:A	20.5832		
1xtl:B	7.8345	1nxz:B	13.7546	1u69:B	20.5832		
1xtl:D	7.8345	1y0h:B	13.9355	1tul:A	20.5931		
1xtl:A	8.0106	1nxz:A	13.9831	2cw5:A	21.0132		
1xtl:C	8.4507	1zp6:A	14.0403	2apl:A	21.1735		
1vhs:B	9.1433	1vhy:A	14.3722	1u69:D	21.6682		
2eui:A	9.1935	1yqe:A	14.4760	1u69:C	21.6802		
1mw7:A	9.2593	1rz3:A	14.5003	1ze0:A	21.6814		
2ean:D	9.2718	1vhy:B	14.5342	1y8t:C	23.0587		
1vhs:A	9.3577	1y0h:A	14.5546	2evr:A	24.9724		
1nc5:A	9.4563	1u7i:A	15.3551	1wu8:A	26.3959		
1y1l:D	9.5055	1wdt:A	15.4850	1wu8:C	26.4467		
1iul:A	9.5903	1vdh:B	15.7635	1wu8:B	26.4975		
1t57:A	9.7037	1rv9:A	15.8516	1yyv:A	31.2357		
1y1l:B	9.7514	1vdh:C	15.9113	1t6s:A	31.6436		
1t8h:A	9.7805	1vdh:E	15.9113	1t6s:B	31.6436		
				1y7m:B	0.1653	1tul:A	16.8040
				1y7m:A	0.2479	2evr:A	17.1271
				1yyv:A	1.3730	1t6s:B	17.2043
				1ze0:A	3.1858	1t6s:A	17.2811
				1y8t:A	5.0660	1nx8:C	17.5465
				1y8t:B	7.2182	1tul:B	17.9934
				1njh:A	8.2450	1zp6:A	18.4466
				1y8t:C	8.9508	1wu8:C	20.2538
				1yey:B	11.5880	1rv9:A	20.4609
				1z6m:A	11.7288	1wu8:A	20.5076
				1y0h:B	11.7419	1wu8:B	20.5076
				1u6l:B	11.7773	1vhs:A	21.3323
				1yey:C	12.0621	1vhs:B	21.5815
				1t8h:A	13.1679	1rlh:A	23.2959
				1y0h:A	13.9272	1zz3:A	23.7753
				1nx4:B	14.4970	1t57:A	24.9630
				1k3r:A	14.7272	1zzm:A	26.7288
				1yqe:A	15.2753	1v6h:B	27.7035
				1vim:C	15.4959	1v6h:A	27.9609
				1k3r:B	15.7163	1v6h:C	28.0488
				1u7i:A	15.9309	1nc5:A	28.7741
				1nx4:C	16.0751	2cw5:A	29.1307
				1nx4:A	16.4959	1mwq:A	30.9976
				1u7i:B	16.5692		

[NOTE: only structures w/ CPM and TSM values within 10.0 units of those of the training structures are shown]

1k3r	A-32	H-83	L-30	R-33	AAAA	1vhs	A-104	C-91	L-3	R-106	AAAA
1k3r	A-32	H-83	L-30	R-33	BBBB	1vhs	A-104	C-91	L-3	R-106	BBBB
1mwq	A-26	H-0	L-31	R-27	AAAA	1vim	A-51	H--2	L-56	R-55	CCCD*
1nc5	A-36	C-48	L-73	R-38	AAAA	1wu8	A-77	H-36	F-132	R-75	AAAA
1njh	A-11	H-24	L-92	R-15	AAAA	1wu8	A-77	H-36	F-132	R-75	BBBB
1nx4	A-119	H-251	L-265	R-264	AAAA	1wu8	A-77	H-36	F-132	R-75	CCCC
1nx4	A-119	H-251	L-265	R-264	BBBB	1y0h	A-24	C-39	L-26	R-23	AAAA
1nx4	A-119	H-251	L-265	R-264	CCCC	1y0h	A-24	C-39	L-26	R-23	BBBB
1nx8	A-119	H-251	L-265	R-264	CCCC	1y8t	A-137	H-49	F-206	R-140	AAAA
1rlh	A-5	C-94	L-78	R-80	AAAA	1y8t	A-137	H-49	F-206	R-140	BBBB
1rv9	A-172	H-135	F-173	R-240	AAAA	1y8t	A-137	H-49	F-206	R-140	CCCC
1rz3	A-99	H-57	L-97	R-22	AAAA	1yey	A-380	H-285	L-320	R-379	BBBB
1t57	A-45	C-6	L-20	R-47	AAAA	1yey	A-380	H-285	L-320	R-379	CCCC
1t6s	A-131	H-161	L-134	R-132	AAAA	1yqe	A-172	H-76	L-120	R-123	AAAA
1t6s	A-131	H-161	L-134	R-132	BBBB	1yyv	A-104	H-28	L-38	R-42	AAAA
1t8h	A-25	C-242	F-5	R-14	AAAA	1z6m	A-100	H-81	F-99	R-40	AAAA
1tul	A-110	H-7	L-112	R-107	AAAA	1ze0	A-146	H-104	F-147	R-148	AAAA
1tul	A-110	H-7	L-112	R-107	BBBB	1zp6	A-145	C-123	F-144	R-113	AAAA
1u6l	A-32	H-25	L-58	R-57	BBBB	1zzm	A-195	H-157	L-197	R-237	AAAA
1u7i	A-30	H-62	L-56	R-55	AAAA	2cw5	A-79	H-38	F-138	R-77	AAAA
1u7i	A-30	H-62	L-56	R-55	BBBB	2evr	A-39	C-31	L-25	R-42	AAAA
1v6h	A-21	H-62	L-27	R-70	AAAA						
1v6h	A-21	H-62	L-27	R-70	BBBB						
1v6h	A-21	H-62	L-27	R-70	CCCC						

Table 5 (part 4 of 7)

heme-bound Nitric Oxide-binding proteins

CPM		TSM	
1zol:B	19.6326	1zol:A	6.7738
lozw:A	20.3294	1xk3:A	6.9994
1zol:A	20.6659	1zol:B	7.2905
1xk3:A	20.9409	lozw:A	7.6661
1zbr:A	2.2095	* 1qvw:B	11.2707
1zbr:B	2.2095	* 1xtm:A	11.2875
1xby:A	5.3211	* 1qvw:A	11.3063
1xbv:B	5.3922	* 1xtl:B	14.3486
1xbx:A	5.3955	* 1xtl:C	14.5246
1xby:B	5.4021	* 1xtl:A	14.6127
1xbx:B	5.4154	* 1xtl:D	14.6127
1xbz:B	5.5215	* 1xqb:A	15.6164
liuk:A	6.4279	* 1xqb:B	15.6849
1tt4:A	6.5303	* 1o61:B	17.2366
1qy9:A	7.2523	* 1o69:B	17.2473
2a67:D	7.3117	* 2f9c:A	18.0137
1qy9:D	7.4473	* 2f9c:B	18.6037
2a67:A	7.4492	* 1zsw:A	18.7040
1qy9:B	7.4775	* 1xcc:B	19.4334
1qya:A	8.0950	* 1xcc:A	19.4460
* 1u9c:A	9.5460	* 1xcc:C	19.6034
* 1qvz:A	10.3853	* 1xcc:D	19.9082
* 1qvz:B	10.4966	* 1vkh:B	22.4164
* 1zbs:A	10.5114	* 1uan:A	23.8290
* 1qvv:C	10.8514	* 1uan:B	23.8683
* 1qvv:A	10.8939	* 2b4w:A	24.7971
* 1rw7:A	10.9505	* 2arz:B	28.7582
* 1qvv:B	10.9945	* 2arz:A	29.6158
* 1xe8:A	11.0664	* 1wdt:A	30.3272
* 1qvv:D	11.2290		
		* 2arz:A	1.7076
		* 1wdt:A	1.7920
		* 2arz:B	2.1786
		* 1vkh:B	4.6930
		* 2b4w:A	5.9513
		* 1uan:A	9.4262
		* 1uan:B	9.5238
		* 1zsw:A	10.2977
		* 1xe8:A	11.8042
		* 1xtl:A	17.0775
		* 1xtl:B	17.0775
		* 1xtl:D	17.0775
		* 1xtl:C	17.1655
		* 1xqb:A	17.6712
		* 1xqb:B	17.6712
		1o69:B	18.1097
		1o61:B	18.2038
		2a67:D	19.3501
		2a67:A	19.4883
		1u9c:A	25.9022
		1qvv:D	28.3240
		1rw7:A	28.7382
		1qvv:A	28.8268
		1qvw:A	29.2536
		1qvw:B	29.3370
		1qvv:C	29.3823
		1xtm:A	29.9824
		1tt4:A	30.0682
		1qvz:A	30.1508
		1qvz:B	30.2762
		2f9c:B	30.3874
		1qvz:B	30.4176
		1zbs:A	30.6818
		2f9c:A	32.4889
		1xcc:A	36.9135
		1xcc:D	36.9478
		1xcc:B	36.9972
		1xcc:C	37.4504
		1xbx:A	50.2146
		1xby:A	50.7034
		1qya:A	51.1219
		1xbx:B	51.2000
		1xby:B	51.3812
		1xbz:B	52.4540
		1xbv:B	52.5123
		1qy9:B	52.6126
		1qy9:D	52.8039
		1qy9:A	52.9730
		liuk:A	55.1882
		1zbr:B	66.8571
		1zbr:A	68.8762

heme-NO-binding proteins (cont'd.)

1o61	G-350	C-101	F-80	H-336	BBBB
1o69	G-350	C-101	F-80	H-336	BBBB
1qvv	G-25	H-108	F-17	Y-13	AAAA
1qvv	G-25	H-108	F-17	Y-13	BBBB
1qvv	G-25	H-108	F-17	Y-13	CCCC
1qvv	G-25	H-108	F-17	Y-13	DDDD
1qvw	G-25	H-108	F-17	Y-13	AAAA
1qvw	G-25	H-108	F-17	Y-13	BBBB
1qvz	G-25	H-108	F-17	Y-13	AAAA
1qvz	G-25	H-108	F-17	Y-13	BBBB
1rw7	G-25	H-108	F-17	Y-13	AAAA
1u9c	G-22	H-96	F-100	H-12	AAAA
* 1uan	G-20	C-18	F-213	R-198	AAAA
* 1uan	G-20	C-18	F-213	R-198	BBBB
* 1vkh	G-112	H-36	F-50	H-109	BBBB
* 1wdt	G-89	H-432	F-87	R-63	AAAA
1xcc	H-39	C-73	F-71	H-79	AAAA
1xcc	H-39	C-73	F-71	H-79	BBBB
1xcc	H-39	C-73	F-71	H-79	CCCC
1xcc	H-39	C-73	F-71	H-79	DDDD
* 1xe8	G-93	H-202	F-178	H-42	AAAA
* 1xqb	G-34	H-120	F-118	H-13	AAAA
* 1xqb	G-34	H-13	F-118	H-120	BBBB
* 1xtl	H-120	H-86	F-114	H-121	AAAA
* 1xtl	H-120	H-86	F-114	H-121	BBBB
* 1xtl	H-120	H-86	F-114	H-121	CCCC
* 1xtl	H-120	H-86	F-114	H-121	DDDD
1xtm	G-123	H-112	F-114	H-120	AAAA
1zbs	G-100	C-106	F-125	Y-277	AAAA
* 1zsw	H-46	H-9	F-256	R-253	AAAA
* 2arz	H-201	C-40	F-110	Y-17	AAAA
* 2arz	H-201	C-40	F-110	Y-17	BBBB
* 2b4w	G-191	C-205	F-148	R-136	AAAA
2f9c	G-212	H-213	F-191	R-215	AAAA
2f9c	G-212	H-213	F-191	R-215	BBBB

Table 5 (part 5 of 7)

Unbound Nitric Oxide-binding proteins

CPM			TSM		
1zgn:B	25.5828		1zgn:A	5.7669	
1zgn:A	26.2577		1zgn:B	5.8896	
1xa0:A	1.9108		* 1uc2:A	10.9604	
1xa0:B	2.0976		* 1vim:B	13.3798	
1tzz:A	5.5058		* 1tzz:B	15.7609	
1tzz:B	6.4538		* 1zn6:A	16.0147	
1wu8:A	7.2081		1tzz:A	17.1025	
1vim:B	13.9373		1vbk:A	19.7980	
* 1uc2:A	14.7380		1vbk:B	20.7846	
* 1zn6:A	15.0978		1wu8:A	62.0812	
* 1vbk:B	20.0751		1xa0:B	93.1935	
* 1vbk:A	21.0505		1xa0:A	94.8195	
1tzz	Y-2061	R-2060	I-2018	G-2059	BBBB
* 1uc2	Y-451	R-408	I-74	G-407	AAAA
1vbk	Y-8	R-50	I-116	G-49	AAAA
1vbk	Y-8	R-50	I-116	G-49	BBBB
1vim	Y-47	R-44	I-83	G-46	BBBB
* 1zn6	Y-156	R-61	I-153	G-60	AAAA

Table 5 (part 6 of 7)

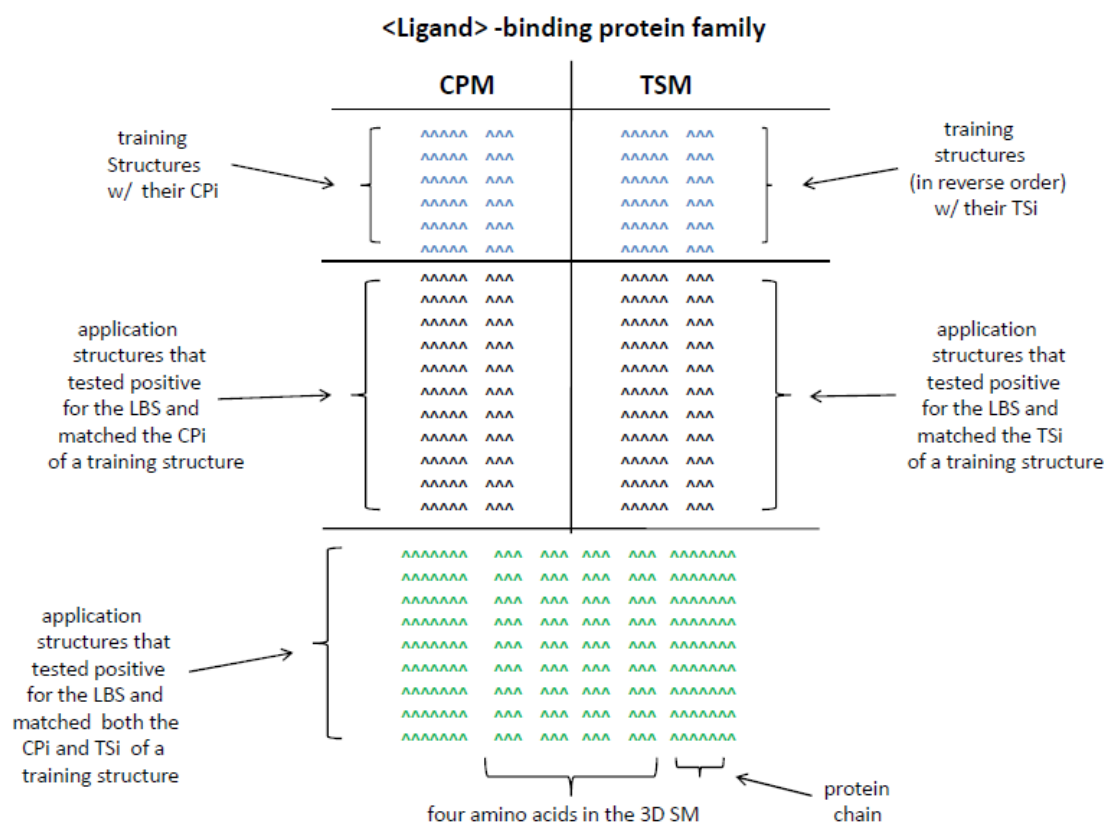


Table 7) 5 (part 7 of

PDB ID	LBS Detected	PDB Header	Source Organism	Remarks	Published Reference
1RU8	GTP ^d	STRUCTURAL GENOMICS, UNKNOWN FUNCTION 11-DEC-03	<i>Pyrococcus furiosus</i>	PUTATIVE N-TYPE ATP PYROPHOSPHATASE; NSG TARGET PFR23	none
1XTL ^a	GTP	STRUCTURAL GENOMICS, UNKNOWN FUNCTION 22-OCT-04	<i>Bacillus subtilis</i>	P104H MUTANT OF HYPOTHETICAL SUPEROXIDE DISMUTASE-LIKE PROTEIN YOJM	none
1FL9	ATP ^e	STRUCTURAL GENOMICS, UNKNOWN FUNCTION 13-AUG-00	<i>Haemophilus influenzae</i>	THE YJEE PROTEIN: HYPOTHETICAL PROTEIN HI0065 A NUCLEOTIDE-BINDING FOLD, A PUTATIVE ATPASE INVOLVED IN CELL WALL SYNTHESIS	Proteins. 2002 Aug 1;48(2):220-6
1MWW	ATP	STRUCTURAL GENOMICS, UNKNOWN FUNCTION 01-OCT-02	<i>Haemophilus influenzae</i>	STRUCTURE OF THE HYPOTHETICAL PROTEIN HI1388.1 WITH A TAUTOMERASE/MIF FOLD	none
1NF2	ATP	STRUCTURAL GENOMICS/UNKNOWN FUNCTION 12-DEC-02	<i>Thermotoga maritima</i>	PROTEIN TM0651, A PHOSPHATASE with a NEW FOLD AND A UNIQUE SUBSTRATE BINDING DOMAIN	none
1O1Y	ATP	STRUCTURAL GENOMICS, UNKNOWN FUNCTION 12-FEB-03	<i>Thermotoga maritima</i>	CONSERVED HYPOTHETICAL PROTEIN TM1158, A PUTATIVE GLUTAMINE AMIDO TRANSFERASE	Proteins. 2004 Mar 1;54(4):801-5
1RKI	ATP	STRUCTURAL GENOMICS, UNKNOWN FUNCTION 21-NOV-03	<i>Pyrobaculum aerophilum</i>	PROTEIN PAG5_736 WITH THREE DISULFIDE BONDS	PLoS Biol. 2005 Sep;3(9):e309. Epub 2005 Aug 23
1RKQ	ATP	STRUCTURAL GENOMICS, UNKNOWN FUNCTION 23-NOV-03	<i>Escherichia coli</i>	NYSGRC TARGET T1436: HYPOTHETICAL PROTEIN YIDA TWO-DOMAIN STRUCTURE W/ BETA-ALPHA SANDWICH; CONTAINS MG++	none
1T57	ATP	STRUCTURAL GENOMICS, UNKNOWN FUNCTION 03-MAY-04	<i>Methanobacterium thermoautotrophicum</i>	CONSERVED PROTEIN MTH1675	none
1TQ8	ATP	STRUCTURAL GENOMICS, UNKNOWN FUNCTION 18-JUN-04	<i>Mycobacterium tuberculosis H37RV</i>	HYPOTHETICAL PROTEIN RV1836, NYSGRC TARGET T1533	none
1WM6	ATP	STRUCTURAL GENOMICS, UNKNOWN FUNCTION 04-JUL-04	<i>Thermus thermophilus HB8</i>	PROTEIN TT0310: A PHENYLACETIC ACID DEGRADATION PROTEIN PAAI; THIOESTERASE W/ HOT DOG FOLD	J Mol Biol. 2005 Sep 9;352(1):212-28
2CVL	ATP	STRUCTURAL GENOMICS, UNKNOWN FUNCTION 08-JUN-05	<i>Thermus thermophilus HB8</i>	PROTEIN TTHA0137: A PROTEIN TRANSLATION INITIATION INHIBITOR	none
1IUU	sialic acid	STRUCTURAL GENOMICS, UNKNOWN FUNCTION 05-MAR-02	<i>Thermus thermophilus</i>	HYPOTHETICAL PROTEIN TT1468, A CONSERVED COA- BINDING PROTEIN	none
1SQH	sialic acid	STRUCTURAL GENOMICS, UNKNOWN FUNCTION 18-MAR-04	<i>Drosophila malonogaster</i>	HYPOTHETICAL PROTEIN CG14615-PA (Q9VR51), NSGC TARGET FR87	none
1VKA	sialic acid	STRUCTURAL GENOMICS, UNKNOWN FUNCTION 10-MAY-04	<i>Homo sapiens</i>	HYPOTHETICAL PROTEIN Q15691: N-TERMINAL FRAGMENT MICROTUBULE-ASSOCIATED PROTEIN RPIEB FAMILY; SYN.: APC-BINDING PROTEIN EB1	none
1Y6Z	sialic acid	STRUCTURAL GENOMICS, UNKNOWN FUNCTION 07-DEC-04	<i>Plasmodium falciparum</i>	C-TERMINAL DOMAIN OF PUTATIVE HEAT SHOCK PROTEIN PF14_0417 (CHAPERONE)	none
1NJH	retinoic acid	STRUCTURAL GENOMICS, UNKNOWN FUNCTION 31-DEC-02	<i>Bacillus subtilis</i>	THE YOJF PROTEIN	none
1NX4	retinoic acid	UNKNOWN FUNCTION, 08-FEB-03	<i>Erwinia carotovora</i>	CARBAPENEM SYNTHASE (CARC) W/ JELLY ROLL FOLD	J Biol Chem. 2003 Jun 6;278(23):20843-50. Epub 2003 Feb 28
1NX8	retinoic acid	UNKNOWN FUNCTION, 10-FEB-03	<i>Erwinia carotovora</i>	CARBAPENEM SYNTHASE (CARC) WITH JELLY ROLL FOLD COMPLEXED WITH N-ACETYL PROLINE	J Biol Chem. 2003 Jun 6;278(23):20843-50. Epub 2003 Feb 28
1RLH	retinoic acid	STRUCTURAL GENOMICS, UNKNOWN FUNCTION 25-NOV-03	<i>Thermoplasma acidophilum</i>	A CONSERVED HYPOTHETICAL PROTEIN FROM GENE CAC12474;	none
1RV9	retinoic acid	UNKNOWN FUNCTION, 13-DEC-03	<i>Neisseria meningitidis</i>	A CONSERVED HYPOTHETICAL PROTEIN NMB0708 W/ ALPHA-BETA-BETA-ALPHA STRUCTURE	none
1TU1	retinoic acid	STRUCTURAL GENOMICS, UNKNOWN FUNCTION 24-JUN-04	<i>Pseudomonas aeruginosa</i>	HYPOTHETICAL PROTEIN PA0094	none
1U6L	retinoic acid	UNKNOWN FUNCTION, 30-JUL-04	<i>Pseudomonas aeruginosa</i>	HYPOTHETICAL PROTEIN	none
1VIM	retinoic acid	STRUCTURAL GENOMICS, UNKNOWN FUNCTION 01-DEC-03	<i>Archaeoglobus fulgidus</i>	HYPOTHETICAL PROTEIN AF1766	J Neurochem. 2000 Oct;75(4):1475-86

1WU8	retinoic acid	STRUCTURAL GENOMICS, UNKNOWN FUNCTION 02-OCT-04	<i>Pyrococcus horikoshii</i> OT3	HYPOTHETICAL PROTEIN PH483	none
1YST	retinoic acid	UNKNOWN FUNCTION, 13-DEC-04	<i>Mycobacterium</i> <i>tuberculosis</i> <i>Xanthomonas</i>	PROTEOLYTICALLY ACTIVE FORM OF HYPOTHETICAL PROTEIN RV6993, A SERINE PROTEASE-INTRA HOMOLOG	none
1YEY	retinoic acid	STRUCTURAL GENOMICS, UNKNOWN FUNCTION 26-DEC-04	<i>Campestris</i> PV. Str. ATCC 33913	L-FUCONATE DEHYDRATASE	none
1Z0M	retinoic acid	STRUCTURAL GENOMICS, UNKNOWN FUNCTION 23-MAR-05	<i>Enterococcus faecalis</i> V593	CONSERVED HYPOTHETICAL PROTEIN	none
2EVR	retinoic acid	STRUCTURAL GENOMICS, UNKNOWN FUNCTION 31-OCT-05	<i>Neisseria meningitidis</i> PC 73102	PROTEIN 5369717, CELL WALL-ASSOCIATED HYDROLASES (INVASION-ASSOCIATED PROTEINS)	none
1UAN	heme-NO	STRUCTURAL GENOMICS, UNKNOWN FUNCTION 12-MAR-03	<i>Thermus</i> <i>marinophilus</i> HB8	CONSERVED HYPOTHETICAL PROTEIN TT1642	none
1VKH	heme-NO	STRUCTURAL GENOMICS, UNKNOWN FUNCTION 23-MAY-04	<i>Saccharomyces</i> <i>cerevisiae</i>	PUTATIVE SERINE HYDROLASE WITH ALPHABETA FOLD(YDR425C)	Protein, 2005 Feb 15;58(3):755-8
1WDT ^a	heme-NO	STRUCTURAL GENOMICS, UNKNOWN FUNCTION 17-MAY-04	<i>Thermus</i> <i>marinophilus</i> HB8	ELONGATION FACTOR G HOMOLOG TT00300905, GTP COMPLEX	none
1XEB	heme-NO	STRUCTURAL GENOMICS, UNKNOWN FUNCTION 06-SEP-04	<i>Saccharomyces</i> <i>cerevisiae</i>	HYPOTHETICAL 22.5 KD PROTEIN YML079W: NEW SEQUENCE FAMILY OF THE JELLY ROLL FOLD; IN TUG1 CPD INTERGENIC REGION; SYNL: YML079W; CLPVI SUPERFAMILY	Protein Sci. 2005 Jan;14(1):209-15
1XQB	heme-NO	STRUCTURAL GENOMICS, UNKNOWN FUNCTION 11-OCT-04	<i>Haemophilus</i> <i>influenzae</i>	NS3C TARGET 1947, HYPOTHETICAL UPF069 PROTEIN H0510; YAGB PROTEIN	none
1XTL ^a	heme-NO	STRUCTURAL GENOMICS, UNKNOWN FUNCTION 25-OCT-04	<i>Bacillus subtilis</i>	P104H MUTANT OF S.O.D.-LIKE HYPOTHETICAL PROTEIN YQUM; CU-ZN SOD	none
1Z5W ^d	heme-NO	STRUCTURAL GENOMICS, UNKNOWN FUNCTION 25-MAY-05	<i>Bacillus cereus</i>	GLYOXALASE FAMILY METALLOPROTEIN	none
2ARZ	heme-NO	UNKNOWN FUNCTION, 23-AUG-05	<i>Pseudomonas</i> <i>aeruginosa</i>	HYPOTHETICAL PROTEIN PA4355	none
2B4W	heme-NO	STRUCTURAL GENOMICS, UNKNOWN FUNCTION 26-SEP-05	<i>Leishmania major</i> (protozoa)	CONSERVED HYPOTHETICAL PROTEIN	none
1UC2	unbound NO	STRUCTURAL GENOMICS, UNKNOWN FUNCTION 06-APR-03	<i>Pyrococcus horikoshii</i> (archaea)	HYPOTHETICAL EXTEN; RTOR HOMOLOG PROTEIN OF PH1802	none
1ZV6	unbound NO	STRUCTURAL GENOMICS, UNKNOWN FUNCTION 11-MAY-05	<i>Bordetella</i> <i>bronchiseptica</i>	PHAGE-RELATED CONSERVED HYPOTHETICAL PROTEIN GTWLM; NS3C TARGET B0710 W/ NOVEL STRUCTURE	none

^a A heme-NO (nitric oxide) 3D SM has also been detected in this structure; see 1XTL^a below.

^b A 3D SM corresponding to monomer 2 in the interleukin-2 homodimer complex (3INK:B) was also detected in this structure (see Reyes, V.M., 2005c).

^c A 3D SM corresponding to monomer 1 in the RAP+RAF1B complex (RAP+Grippnp complexed w/ c-RAF1 Ras-binding domain; 1C1Y:A) was also detected in this structure (see Reyes, V.M., 2005c).

^d The specific GTP LBS detected is the 3D SM corresponding to that in the small, Ras-type G-protein family.

^e The specific ATP LBS detected is the 3D SM corresponding to that in the ser/thr protein kinase family.

Table 6.